This document is the **Accepted Manuscript version** of a Published Work that appeared in final form in **Food Chemistry 260 : 239-273(2018)**

https://doi.org/10.1016/j.foodchem.2018.03.151

© 2018. This manuscript version is made available under the CC-BY-NC-ND 4.0 license https://creativecommons.org/licenses/by-nc-nd/4.0/

Polyphenolic profile of butterhead lettuce cultivar by ultrahigh performance liquid chromatography coupled online to UV–visible spectrophotometry and quadrupole time-of-flight mass spectrometry

Gabriela E. Viacava, Sara I. Roura, Diana M. López-Márquez, Luis A. Berrueta, Blanca Gallo, Rosa M. Alonso-Salces

Food Chemistry 260 : 239-273 (2018)

DOI:10.1016/j.foodchem.2018.03.151

Polyphenolic profile of butterhead lettuce cultivar by ultrahigh performance liquid chromatography coupled online to UV-visible spectrophotometry and quadrupole time-of-flight mass spectrometry

Running title:

Polyphenolic profile of butterhead lettuce by UHPLC-DAD-ESI-QToF/MS^{E}

Gabriela E. Viacava[a], Sara I. Roura[a], Diana M. López-Márquez[b], Luis A. Berrueta[b], Blanca Gallo[b], Rosa M. Alonso-Salces[c,*]

[a] Grupo de Investigación en Ingeniería en Alimentos, CONICET, Departamento de Ingeniería Química y en Alimentos, Facultad de Ingeniería, Universidad Nacional de Mar del Plata, Juan B. Justo 4302, 7600 Mar del Plata, Argentina. E-mail address: gviacava@fi.mdp.edu.ar; sroura@fi.mdp.edu.ar

[b] Departamento de Química Analítica, Facultad de Ciencia y Tecnología, Universidad del País Vasco/Euskal Herriko Unibertsitatea (UPV/EHU), P.O. Box 644, 48080 Bilbao, Spain. E-mail address: lomadianam@gmail.com; luisangel.berrueta@ehu.eus; blanca.gallo@ehu.eus

[c] Departamento de Biología, CONICET, Facultad de Ciencias Exactas y Naturales, Universidad Nacional de Mar del Plata, Funes 3350, 7600 Mar del Plata, Argentina.

* Corresponding author.

E-mail address: rosamaria.alonsosalces@gmail.com

Abstract

In the present study, the butterhead lettuce cultivar was analyzed by ultrahigh performance liquid chromatography (UHPLC) coupled online to diode array detection (DAD), electrospray ionization (ESI) and quadrupole time-of-flight mass spectrometry (QToF/MS) in the positive and negative ion mode in order to characterize its polyphenolic profile for the first time. The instrument acquisition mode MS^E was used to collect automatic and simultaneous information of exact mass at high and low collision energies of precursor ions as well as other ions produced as a result of their fragmentation. One hundred eleven phenolic compounds were identified in the acidified hydromethanolic extract of freeze-dried leaves of butterhead lettuce cultivar: 40 hydroxycinnamic acid derivatives, 21 hydroxybenzoic acid derivatives, 2 hydroxyphenylacetic acid derivatives, 18 flavonols, 9 flavones, one flavanone, 7 coumarins, one hydrolysable tannin and 12 lignans. Forty seven of these compounds have been tentatively identified for the first time in lettuce.

Keywords: *Lactuca sativa*, lettuce, phenolic compounds, UHPLC-QToF, mass spectrometry, MS^E

Chemical compounds studied in this article:

5-Caffeoylquinic acid (PubChem CID: 12310830); caffeoylmalic acid (PubChem CID: 4484594); 4-hydroxyphenylacetic acid (PubChem CID: 127); quercetin-3-*O*-galactoside (PubChem CID: 90657624); quercetin-3-*O*-glucuronide (PubChem CID: 5274585); kaempferol-3-*O*-glucuronide (PubChem CID: 5318759); luteolin 7-glucoside (PubChem CID: 5280637); luteolin 7-rutinoside (PubChem CID: 44258082); esculetin-6-*O*-glucoside (PubChem CID: 5281417); syringaresinol (PubChem CID: 100067).

1. Introduction

Phenolic compounds are secondary plant metabolites ubiquitous in the plant kingdom involved in protection mechanisms against biotic and abiotic stresses, in the regulation of plant growth and development, and in the organoleptic quality of plant-based foods (Dai & Mumper, 2010). Moreover, the intake of phenolic compounds through fruits and vegetables have been proved to provide beneficial effects attributed to their antioxidant capacity against oxidative stress, cancer and cardiovascular diseases, among others (Watson, Preedy, & Zibadi, 2014). Lettuce (*Lactuca sativa* L.) is one of the most popular leafy vegetables. In particular, the butterhead lettuce is one of the most commonly consumed variety worldwide (Agüero, Viacava, Ponce, & Roura, 2013); however, its polyphenolic profile has not been characterized yet to the authors' knowledge. The main classes of phenolic compounds found in different varieties of lettuce are phenolic acids and flavonols, followed by flavones and anthocyanins (only in red varieties) (Alarcón-Flores, Romero-González, Martínez Vidal, & Garrido Frenich, 2016; Marin, Ferreres, Barberá, & Gil, 2015; Pepe, Sommella, Manfra, De Nisco, Tenore, Scopa et al., 2015). Most analytical methods used to determine polyphenols in lettuce are based on high or ultrahigh performance liquid chromatography (HPLC or UHPLC) coupled to diode array detection (DAD) and/or mass spectrometry (MS and MS/MS) (Abu-Reidah, Contreras, Arráez-Román, Segura-Carretero, & Fernández-Gutiérrez, 2013; Alarcón-Flores et al., 2016; Altunkaya & Gökmen, 2009; Llorach, Martínez-Sánchez, Tomás-Barberán, Gil, & Ferreres, 2008; Pepe et al., 2015; Ribas-Agustí, Gratacós-Cubarsí, Sárraga, García-Regueiro, & Castellari, 2011). UHPLC achieves rapid analysis and better peak separation than HPLC, and coupled to ToF or QToF instruments provides a highly attractive analytical technique with very high resolution and accurate mass measurements of the precursor and fragment ions (Ramirez-Ambrosi, Abad-Garcia, Viloria-Bernal, Garmon-Lobato, Berrueta, & Gallo, 2013). This technique has been already used to characterize 95 phenolic compounds in three lettuce cultivars (baby, romaine, and iceberg) (Abu-Reidah et al., 2013). Technological advances such as the so called MS^E data acquisition mode has been successfully used for the structural elucidation of

phenolic compounds in complex plant extracts (Ramirez-Ambrosi et al., 2013). MS^E acquisition method maximizes the QToF instrument duty cycle performing simultaneous collection of precursor ions as well as other ions produced as a result of their fragmentation in exact mass mode over a single experimental run. Since many compounds still remain unidentified in lettuce cultivars and the utilization of analytical edge technology can provide new structural information and allow the identification of unknown polyphenols, the present study exploits the use of UHPLC-DAD-ESI-QToF/MS^E for the characterization of the polyphenolic profile of the butterhead lettuce cultivar, which is here reported for the first time to the authors' knowledge.

2. Materials and Methods

2.1. Reagents, solvents and standards

Water, methanol, acetonitrile, and formic acid (Fisher Scientific, Fair Lawn, NJ, USA) were of Optima® LC/MS grade; ascorbic acid (Panreac, Barcelona, Spain), analytical grade; and glacial acetic acid (Merck, Darmstadt, Germany), Suprapur® quality. Leucine Enkephalin acetate hydrate and sodium formate solution were provided by Sigma-Aldrich Chemie (Steinheim, Germany). Luteolin-7-*O*-glucoside, kaempferol-3-*O*-glucoside, quercetin-3-*O*-galactoside, quercetin-3-*O*-rhamnoside were purchased from Extrasynthèse (Genay, France); caffeoyltartaric acid and quercetin-3-*O*-glucoside, from Chromadex (Irvine, CA, USA); 5-*O*-caffeoylquinic acid, *p*-coumaric acid, 1,5-dicaffeoylquinic acid, 1,3-dicaffeoylquinic acid, and quercetin-3-*O*-rutinoside, from Sigma-Aldrich Chemie (Steinheim, Germany); and ferulic acid, caffeic acid, and 3,4-dihydroxybenzoic acid, from Fluka Chemie (Steinheim,Germany). Standard stock solutions of phenolic compounds were prepared in methanol; and a reference solution of these compounds (5 μg/mL), in methanol-water-acetic acid (30:65:5, v/v/v).

2.2. Plant material

Heads of butterhead lettuce (*Lactuca sativa* var. Lores) were obtained from a local producer in Sierra de los Padres (Mar del Plata, Argentina). Lettuce samples were frozen with liquid nitrogen

and freeze-dried, homogenized and crushed to obtain a homogeneous powder, which was stored at room temperature in dark in a desiccator until analysis.

2.3. Extraction of polyphenols in lettuce

Freeze-dried lettuce (0.1 g) was extracted with 5 mL of methanol-water-acetic acid (30:65:5, v/v/v) containing ascorbic acid (2 g/L) in an ultrasonic bath for 10 min. Then, the extract was centrifuged at 6000 rpm during 15 min at 4 ºC, and the supernatant was filtered through a 0.45 µm PTFE filter (Waters, Milford, CA, USA) prior to injection into the UHPLC system.

2.4. UHPLC-DAD-ESI-QToF/MS^{E}

Lettuce extract was analyzed using an ACQUITY UPLC^{TM} system from Waters (Milford, MA, USA), equipped with a binary solvent delivery pump, an autosampler, a column compartment a PDA detector, and controlled by MassLynx v4.1 software. A reverse phase Acquity UPLC BEH C18 column (2.1 mm × 100 mm, 1.7 µm) and a Acquity UPLC BEH C18 VanGuard^{TM} pre-column (1.7 µm) from Waters (Milford, USA) were used. Flow rate was 0.5 mL/min; injection volume, 5 µL; column and autosampler temperatures, 40ºC and 4 ºC respectively. Mobile phases consisted of 0.1% (v/v) acetic acid in water (A) and 0.1% (v/v) acetic acid in methanol (B). The elution conditions applied were: 0–8.5 min, linear gradient 0–13% B; 8.5–11 min, 13% B isocratic; 11–12.3 min, linear gradient 13–15% B; 12.3–13.8 min, linear gradient 15–19% B; 13.8–17.3 min, linear gradient 19–23% B; 17.3–19 min, 23% B isocratic; 19–24 min, linear gradient 23–30% B; 24–26 min, 30% B isocratic; 26–27 min, linear gradient 30–100% B; 27–28 min, 100% B isocratic; and finally reconditioning of the column with 100% A isocratic. UV-visible spectra were recorded from 210 to 500 nm (20 Hz, 1.2 nm resolution). Hydroxybenzoic acids were monitored at 254 nm; flavanones at 280 nm; hydroxycinnamic acids and coumarins at 320 nm; flavonols and flavones at 370 nm.

All MS data acquisitions were performed on a SYNAPT^{TM} G2 HDMS with a quadrupole time of flight (QToF) configuration (Waters, Milford, MA, USA) equipped with an electrospray ionization (ESI) source operating in both positive and negative modes. The capillary voltage was set

to 0.7 kV (ESI+) or 0.5 kV (ESI−). Nitrogen was used as the desolvation and cone gas at flow rates of 900 L/h and 10 L/h, respectively. The source and desolvation temperatures were 120 ºC and 400 ºC respectively. Leucine-enkephalin solution (2 ng/µL) in 0.1% (v/v) formic acid in acetonitrile-water (50:50, v/v) was used for the lock mass correction (*m/z* 556.2771 and 278.1141, or *m/z* 554.2615 and 236.1035, depending on the ionization mode, were monitored at scan time 0.2 s, interval 10 s, scans to average 3, mass window ± 0.5 Da, cone voltage 30 V, at a flow rate 10 µL/min). Data acquisition was recorded in the mass range 50–1200 *u* in resolution mode (FWHM ≈ 20,000) with a scan time of 0.2 s and an interscan delay of the 0.024 s, and automatically corrected during acquisition based on the lock mass. Before analysis, the mass spectrometer was mass calibrated with the sodium formate solution. To perform MS^E mode analysis, the cone voltage was set to 20 V (ESI+) or 30 V (ESI−) and the quadrupole operated in a wide band RF mode only. Two discrete and independent interleaved acquisition functions were automatically created. The first function, typically set at 6 eV in trap cell of the T-Wave, collects low energy or unfragmented data while the second function collects high energy or fragmented data typically using 6 eV in trap cell and a collision ramp 10–40 eV in transfer cell. In both cases, Argon gas was used for Collision Induced Dissociation (CID). Data were recorded in continuous mode. For instrument control, data acquisition and processing MassLynxTM software Version 4.1 (Waters MS Technology, Milford, USA) was used.

2.5. Identification of phenolic compounds

The identification of the phenolic compounds for which standards were available was carried out by the comparison of their retention times, their UV–vis spectra and MS^E spectra recorded in positive and negative mode with those obtained by injecting standards in the same conditions. The identity of the rest of compounds was elucidated using the following analytical data: *i*) the UV–vis spectrum when it was available to assign the phenolic class (Abad-García, Berrueta, Garmón-Lobato, Gallo, & Vicente, 2009), since each class exhibits a characteristic UV–vis spectrum (Markham, 1982); *ii*) the low collision energy MS^E spectrum in positive and negative ion mode to

150 determine the molecular weight; and since only the protonated/deprotonated molecules are able to
151 form in the electrospray ionization source adducts, clusters and/or molecular complexes with
152 mobile phase species (e.g. adducts with sodium $[M+Na]^+$ at 22 *u* above the protonated molecule,
153 $[2M+Na]^+$ of monoacyl hydroxycinnamic acids, the dehydrated protonated molecule ($[M+H–H_2O]^+$)
154 of phenolic acids and diacyl hydroxycinnamic acids in positive mode; and adducts with
155 HSO_4^- (97 *u*) and AcO^- (43 *u*) and the deprotonated dimer ion $[2M–H]^-$ of monoacyl
156 hydroxycinnamic acid in negative mode), their presence in the low collision energy spectra allows
157 the unequivocal identification of the $[M+H]^+$ or $[M−H]^-$ ions; and *iii*) the high collision energy MS^E
158 spectrum provides the polyphenol fragmentation patterns, which afford structural information
159 related to the type of carbohydrates, the sequence of the glycan part, interglycosidic linkages and
160 the aglycone moiety, allowing to assign the protonated aglycone $[Y_0]^+$ and/or the deprotonated
161 aglycone $[Y_0]^-$. The identification of the aglycone was carried out based on the observation of $^{i,j}A^+$
162 and $^{i,j}B^+$ ions (Ma, Li, Van den Heuvel, & Claeys, 1997). Furthermore, the chromatographic elution
163 order aided in some structural assignments, as well as bibliographic references. IUPAC
164 nomenclature and recommended numbering system (Lozac'h, 1975) were used for chlorogenic
165 acids and flavonoids; and common names were used for other phenolic acid derivatives, coumarins,
166 hydrolysable tannins and lignan derivatives. Structures of each family of compounds studied are
167 presented in Fig. 1.

168 **3. Results and Discussion**

169 A total of 111 phenolic compounds were tentatively identified in the butterhead lettuce
170 cultivar by UHPLC-DAD-ESI-QToF/MS^E. The UV-visible and MS spectral data are summarized in
171 Table 1. DAD and MS chromatograms are shown in Figs. 1S-5S (supplementary material). The
172 high and low energy function MS spectra of compounds from the different phenolic families
173 detected in this cultivar are displayed in Figs. 2 and 3, and in Figs. 6S-9S (supplementary material).

174 **3.1. Phenolic acid derivatives**

For the identification of phenolic acid derivatives, mainly negative ion mode mass spectra were taken into account, although the positive ion mode was used for verification. In the high collision energy MS spectra, losses of H_2O, CO_2 and CO were regularly observed, which have also been described by other authors using IT, QqQ, and QToF (Gómez-Romero, M., Segura-Carretero, & Fernandez-Gutierrez, 2010; Ramirez-Ambrosi et al., 2013).

3.1.1. Hydroxycinnamic derivatives

3.1.1.1. Caffeoylquinic acids

Three major chromatographic peaks (**1**, **3**, **6**), presenting the same UV spectra as the standard *trans*-5-caffeoylquinic acid (*trans*-5-CQA), were detected in the chromatograms extracted from the Total Ion Current (TIC) MS scan chromatogram in negative and positive modes at *m/z* 353 and 355 respectively, which were due to three caffeoylquinic acid (CQA) isomers (Fig. 2S in the supplementary material). Compound **3** (Rt= 7.32 min, λmax= 300, 324 nm) was identified unambiguously as *trans*-5-caffeoylquinic acid by comparison with its standard: the deprotonated molecule $[M-H]^-$ at *m/z* 353 yielded fragment ions at *m/z* 191, 173 and 135; and the protonated molecule $[M+H]^+$, at *m/z* 163 and 145. Moreover, its sodium adducts, $[M+Na]^+$ and $[2M+Na]^+$ at *m/z* 377 and 731 respectively, were also observed (Fig. 6S in the supplementary material). Compounds **1** (Rt= 4.74 min, λmax= 301, 323 nm) and **6** (Rt= 10.23 min, λmax= 301, 316 nm) had the same fragmentation pattern as 5-CQA, and their *m/z* values for $[M+H]^+$ and $[M-H]^-$ were confirmed with the sodium adduct at *m/z* 377 in positive ionization mode, and the $[2M-H]^-$ ion at *m/z* 707 in negative mode. All three peaks (**1**, **3**, **6**) yielded the same base peak at *m/z* 191 due to the deprotonated quinic moiety in the negative high energy function. None of the peaks yielded an intense fragment ion at *m/z* 173 ($[\text{quinic acid}–H–H_2O]^-$). This dehydrated ion of quinic acid is characteristically formed in the negative ion mode when the cinnamoyl group is bonded to the quinic moiety at position 4, as already noted by other authors using other QqQ/MS (Alonso-Salces, Guillou, & Berrueta, 2009) or IT/MS (Clifford, Johnston, Knight, & Kuhnert, 2003). Peak **1** also gave intense ions from the caffeoyl moiety ($[\text{caffeic acid}–H–CO_2]^-$) at *m/z* 135 (71% relative

abundance (RA)) and ([caffeic acid–H]$^-$) at *m/z* 179 (32% RA), characteristic intense ions of the fragmentation pattern of 3-CQA by QqQ/MS (Alonso-Salces et al., 2009). The relative hydrophobicity of cinnamoyl derivatives depends on the position, the number and the identity of the cinnamoyl residues. In general, those chlorogenic acids (CGAs) with a greater number of free equatorial hydroxyl groups in the quinic acid are more hydrophilic than those with a greater number of free axial hydroxyl groups (Clifford, Knight, & Kuhnert, 2005). Taking into account the fact that the hydroxyl groups in the quinic acid are axial in position 1 and 3, and equatorial in positions 4 and 5 (Clifford, Knight, Surucu, & Kuhnert, 2006), the elution order observed for monoacyl-CGAs on C18 reversed-phase LC is 3-CGA, 5-CGA and 4-CGA. This empirical rule was observed by several authors (Abu-Reidah et al., 2013; Alonso-Salces et al., 2009; Clifford et al., 2003). So, isomers substituted in position 3 were the most hydrophilic; and in position 4 the most hydrophobic, although in some packings 4-CQA precedes 5-CQA. On the other hand, the ease of removal of the caffeoyl residue during fragmentation is 1 ≈ 5 > 3 > 4 (Clifford et al., 2005). In the negative low energy function, the base peaks were [M−H]$^-$ at *m/z* 353 for peak **1**, and [quinic acid–H]$^-$ at *m/z* 191 for peaks **3** and **6**, revealing that the caffeoyl moiety in peak **1** was bonded to the quinic structure in a stronger position. So, peak **1** was tentatively assigned to a 3-CQA isomer.

Besides the three major peaks (**1, 3, 6**), other four caffeoylquinic acid isomers (**2**, Rt= 6.65 min; **4**, Rt= 8.12 min; **5**, Rt= 8.36 min; **7**, Rt= 15.06 min) were detected in the chromatograms extracted at *m/z* 353 (ESI–) and 355 (ESI+), presenting the same fragmentation pattern in the positive mode as the former isomers. Chlorogenic acid isomers 1-CQA, 3-CQA (neochlorogenic acid), *cis*-3-CQA, 4-CQA (cryptochlorogenic acid), *cis*-4-CQA and *cis*-5-CQA have been previously found in different *Asteraceae* species (Clifford, Wu, Kirkpatrick, & Kuhnert, 2007; Jaiswal, Kiprotich, & Kuhnert, 2011). In the negative low energy function, compounds **2**, **4** and **7** yielded the deprotonated molecule [M−H]$^-$, whereas all four peaks presented the same base peak at *m/z* 191 due to the deprotonated quinic moiety in the negative high energy function. Furthermore, peak **4** yielded ions at *m/z* 135 (21% RA) and at *m/z* 179 (12% RA); and peak **5**, at *m/z* 173 (13%

RA), whereas for all other isomers, this ion was less than 4% RA. Peak **5,** presenting the most intense *m/z* 173 and eluting later than 5-CQA (**3**), was ascribed to a 4-CQA isomer.

It is widely accepted that *trans* isomers are the substrates and products of the main phenylproponanoid biosynthetic pathway, being the predominant species detected in plant tissues. However it is also known that conversion to the *cis* form occurs readily, especially after exposure to UV light, and therefore *cis* isomers might reasonably be expected in plant extracts (Clifford, Kirkpatrick, Kuhnert, Roozendaal, & Salgado, 2008). Indeed, *cis*-3-CQA, *cis*-4-CQA and *cis*-5-CQA have been previously found in different *Asteraceae* species (Clifford et al., 2005; Clifford et al., 2007; Jaiswal et al., 2011). *Cis* isomers fragment identically to the more common *trans* isomers, however *cis* and *trans* isomers are easily resolved by chromatography. *Cis*-5-acyl and *cis*-1-acyl CGAs are more hydrophobic, thus elute later than their *trans* isomers, whereas the opposite happens with *cis*-3-acyl and *cis*-4-acyl CGAs on endcapped C18 and phenylhexyl packings (Clifford et al., 2008). These observations helped to tentatively identify some compounds. Thus, peak **6** was attributed to *cis*-5-CQA, taking into account the elution order of *cis* and *trans* isomers; the fact that absorption maximum for *cis*-CGA occurs at shorter wavelength than for their *trans* form (Dawidowicz & Typek, 2011); and that it is a major peak as its *trans* isomer. Peaks **1** and **4**, which showed similar fragmentation patterns, were designated to the *trans* and *cis* isomers of 3-CQA respectively.

Peak **2** showed a similar fragmentation pattern to peaks **3** and **6**. Indeed, 1-CQA and 5-CQA are not possible to be reliably distinguished by their fragmentation (Clifford et al., 2005). Fortunately, *trans*-5-CQA is readily available from commercial sources, and 1-CQA can be easily resolved in the chromatographic elution from this, so, in practice, discrimination is straightforward. Peak **2** eluted earlier than *trans*-5-CQA (**3**) and was assigned to a 1-acyl isomer. The remaining peak (**7**) eluted the latest of all CQA, therefore it was ascribed to the other 4-CQA isomer.

Taking into account all the above considerations, the chromatographic peaks were tentatively identified as: **1**, *trans*-3-CQA; **2**, *trans*-1-CQA; **3**, *trans*-5-CQA; **4**, *cis*-3-CQA; **5**, *trans*-4-CQA; **6**,

cis-5-CQA; and **7**, *cis*-4-CQA. Only three CQA isomers had been reported previously in green lettuce, i.e. 5-CQA, 3-CQA and an unidentified CQA isomer (Abu-Reidah et al., 2013; Jeong, Kim, Lee, Kim, Kang, Jin et al., 2015). *trans*-5-CQA (**3**) was the major phenolic compound in butterhead lettuce, as occurs in other green lettuce cultivars (Llorach et al., 2008; Ribas-Agustí et al., 2011; Sobolev, Brosio, Gianferri, & Segre, 2005). The following major CQAs were *cis*-5-CQA and *trans*-3-CQA (20% and 8% of the total intensity of *trans*-5-CQA).

3.1.1.2. p-Coumaroylquinic acids

Compounds **8** (Rt= 9.82 min, λmax= 312 nm) and **9** (Rt= 13.74 min, λmax= 308 nm) were identified as *p*-coumaroylquinic acid isomers on the basis of mass spectral data and UV spectra, which followed the pattern of the *p*-coumaric acid standard. In both low and high energy positive ion mode, the sodium adduct $[M+Na]^+$ at *m/z* 361 was the base peak for both compounds, and the ion at *m/z* 147 ($[p\text{-coumaroyl}+H]^+$) was the secondary most intense ion. In the negative low energy function, the base peaks were $[M-H]^-$ at *m/z* 337 for peak **8** (Fig. 3S in the supplementary material), and $[\text{quinic acid}-H]^-$ at *m/z* 191 for peak **9**, revealing that the *p*-coumaroyl moiety in peak **8** was bonded to the quinic structure in a stronger position. Moreover, peak **8** yielded in the high energy function an intense ion at *m/z* 119 due to its decarboxylation product $[p\text{-coumaric acid-H-}CO_2]^-$, which is characteristic of the fragmentation pattern of 3-*p*-coumaroylquinic acid, thus this isomer was tentatively assigned to peak **8,** for the first time in lettuce cultivars. The base peak of compound **9** at *m/z* 191 due to the deprotonated quinic moiety is characteristic of 5-*p*-coumaroylquinic acid (Clifford et al., 2003). Similarly to CQA isomers, the elution order of both isomers on endcapped C18 packings agrees with these tentatively assignments. 5-*p*-coumaroylquinic acid and an unidentified isomer have been previously reported in bibliography in green lettuce cultivars (Abu-Reidah et al., 2013; Ribas-Agustí et al., 2011).

3.1.1.3. Caffeoyltartaric acid

A caffeoyltartaric acid (peak **10**: Rt= 9.06 min, λmax= 301, 323 nm) was detected in the extracted MS chromatogram set at 311 in the negative ion mode (Fig. 3S in the supplementary

material), presenting the corresponding fragmentation pattern: The dehydrated protonated molecule at *m/z* 293 was the base peak in low energy function; and intense fragments of the deprotonated tartaric (*m/z* 149) and caffeic (*m/z* 179) acids and the losses of water (*m/z* 293) and CO_2 (*m/z* 135; base peak) were observed in the high energy function. Two isomers of caffeoyltartaric acid have been already reported in lettuce in literature (Abu-Reidah et al., 2013; Jeong et al., 2015; Lin, Harnly, Zhang, Fan, & Chen, 2012; Ribas-Agustí et al., 2011; Santos, Oliveira, Ibáñez, & Herrero, 2014).

3.1.1.4. p-Coumaroyltartaric acid

Peak **11** (Rt= 15.63 min, λmax= 310 nm), detected in the extracted MS chromatogram set at *m/z* 295 in the negative ion mode, yielded the base peak at *m/z* 163 due to the deprotonated *p*-coumaric acid, and two fragments at *m/z* 149 (50% RA) and *m/z* 119 (60% RA) due to the deprotonated tartaric acid and the decarboxylation of *p*-coumaric acid in the low energy function. Thus, compound **11** was tentatively identified as *p*-coumaroyltartaric acid, which has been previously found in green lettuce cultivars (Abu-Reidah et al., 2013; Ribas-Agustí et al., 2011).

3.1.1.5. Caffeoylmalic acid

Caffeoylmalic acid (CMA) (peak **12**: Rt= 9.05 min, λmax= 301, 323 nm) was detected when the *m/z* value for the extracted MS chromatogram was set at 295 (negative ion mode) or 297 (positive ion mode). Besides the UV spectra of peak **12** followed the pattern of caffeic acid standard. In the negative ion mode, the high energy function provided ions corresponding to malic acid: the base peak at *m/z* 133 was due to the deprotonated malic moiety; and fragment ions, to the losses of water and CO at *m/z* 115 and 105 respectively. MS^E experiments in the positive ion mode showed that CMA behaved as described above for CQA, yielding the same ions from the caffeoyl moiety, as well as the sodium adduct. CMA has been described before in different lettuce cultivars (Abu-Reidah et al., 2013; Lin et al., 2012; Ribas-Agustí et al., 2011; Santos et al., 2014).

3.1.1.6. Dicaffeoylquinic acids and caffeoylquinic acid glycosides

Both dicaffeoylquinic acids (diCQA) and caffeoylquinic acid-hexosides present an average molecular mass of 516 *u*, and produce isobaric deprotonated or protonated molecules at *m/z* 515 and 517 in the negative and positive ion modes respectively. Five peaks were detected in the extracted MS chromatograms at these *m/z* values: peak **13** (Rt= 5.86), peak **14** (Rt= 7.56), peak **15** (Rt= 20.20, λmax= 321 nm), peak **16** (Rt= 20.63, λmax= 326 nm) and peak **17** (Rt= 24.17, λmax= 331 nm). Based on their accurate masses and fragmentation patterns, these peaks were distinguished as either di-caffeoylquinic acids (**15**, **16** and **17**) with monoisotopic $[M-H]^-$ at *m/z* 515.1190 ($C_{25}H_{23}O_{12}$) and monoisotopic $[M+H]^+$ at *m/z* 517.1346 ($C_{25}H_{25}O_{12}$), and caffeoylquinic acid-hexosides (**13** and **14**) with monoisotopic $[M-H]^-$ at *m/z* 515.1401 ($C_{22}H_{27}O_{14}$) and monoisotopic $[M+H]^+$ at *m/z* 517.1548 ($C_{22}H_{29}O_{14}$), in the negative and positive ion modes respectively.

It is worth to note that the first fragments of the diCQA were due to the loss of one of the caffeoyl moieties, leading to the precursor ion of a CQA (Fig. 2S in the supplementary material); therefore, subsequent fragmentation of these ions yielded the same fragments as the corresponding CQA. In the positive low energy function, the sodium adducts at *m/z* 539 and the dehydrated protonated molecule at *m/z* 499 were detected with different % RA: peak **15**, $[M+H-H_2O]^+$ base peak and $[M+Na]^+$ 80% RA; peak **16**, $[M+Na]^+$ base peak and $[M+H-H_2O]^+$ 20% RA; and peak **17**, $[M+Na]^+$ base peak and $[M+H-H_2O]^+$ 90% RA. The positive high energy function gave a base peak at *m/z* 163 ([caffeic acid+H$-H_2O]^+$) for the three peaks, but $[M+Na]^+$ presented 50% RA for peak **15**, 35% RA for peak **16**, and 70% RA for peak **17**. The % RA differences between these ions are related to the difficulty of removing the acylating residue at the different positions. In accordance with this, the negative low energy function MS spectra disclosed that peak **17** yielded only the deprotonated molecule (*m/z* 515) as the base peak; peak **15**, the base peak $[M-H]^-$ and the fragment $[CQA-H]^-$ ion at *m/z* 353 with 65% RA; and peak **16**, the base peak $[CQA-H]^-$ at *m/z* 353 and $[M-H]^-$ with 40% RA. Hence, these observations suggest that peak **17** contains a caffeoyl moiety at the positions more difficult to be removed ($4 > 3 > 5 \approx 1$) (Clifford et al., 2003; Clifford et al., 2005) than the other peaks, followed by peak **15**. Indeed, the presence of the dehydrated quinic

residue ion [quinic acid–H–H_2O]$^-$ at *m/z* 173 as the base peak in the high negative energy spectra of peak **17** revealed that one of the caffeoyl moieties was bonded to quinic acid at position 4. Then it remained to be determined if the other caffeoyl moiety was substituted at position 1, 3 and 5. Finally, taking also into account the elution order of diCQA isomers (retention time on endcapped C18 packings: 1,3-diCQA <<< 1,4-diCQA << 3,4-diCQA < 1,5-diCQA < 3,5-diCQA << 4,5-diCQA) reported in bibliography (Alonso-Salces et al., 2009; Clifford et al., 2005), compound **17** was assigned to 4,5-diCQA. In the high negative energy function, base peaks of compounds **15** and **16** were [quinic acid–H]$^-$ at *m/z* 191, whereas the characteristic fragment at *m/z* 173 corresponding to the dehydrated quinic residue ion was not detected. Therefore, caffeoyl moieties were substituted at position 1, 3 and 5. Compound **15** was identified unambiguously as 1,5-diCQA by comparison with its standard. Thus, regarding its retention time and the ease of removal of the caffeoyl residue, compound **16** was assigned to 3,5-diCQA. Isomers 3,5-diCQA (isochlorogenic acid A), *cis*-3,5-diCQA, and 4,5-diCQA (isochlorogenic acid B) have previously been reported in *L. sativa* (Abu-Reidah et al., 2013; Lin et al., 2012; Llorach et al., 2008; Ribas-Agustí et al., 2011). Among these, isochlorogenic acid A was reported to be the most abundant in lettuce, as found in the present study, which supported the assignment of compound **16** (Jeong et al., 2015; Mai & Glomb, 2013; Romani, Pinelli, Galardi, Sani, Cimato, & Heimler, 2002). 1-acyl CGA have been found in some Asteraceae (Clifford et al., 2005), however the isomer 1,5-diCQA is reported in lettuce here for the first time.

Caffeoylquinic acid-hexosides (**13** and **14**) base peaks were their sodium adducts in the positive ion mode and the deprotonated molecule in the negative ion mode, which confirmed their identities. The presence of the fragment ion at *m/z* 353 due to the deprotonated CQA, and the base peak at *m/z* 191 due to the deprotonated quinic acid in the negative high energy function of peak **13** also support the assignment. Peak **14** was at trace levels, not being possible to register its fragmentation pattern. To the authors' knowledge, caffeoylquinic acid-hexosides have not been reported in lettuce before.

3.1.1.7. p-Coumaroylcaffeoylquinic acids

Two chromatographic peaks showed protonated and deprotonated molecules that corresponded to *p*-coumaroylcaffeoylquinic acids, at *m/z* 501 in the positive ion mode and at *m/z* 499 in the negative mode: peak **18 (**Rt= 23.58 min, λmax= 312 nm) and peak **19** (Rt= 23.95 min, λmax= 316 nm). In the positive high energy function, the base peaks yielded by both isomers were the fragment ion at *m/z* 147 due to $[p\text{-coumaroyl+H}]^+$, disclosing that the *p*-coumaroyl moiety was attached to the quinic acid in a weaker position than the caffeoyl one. This was also supported by the fragmentation pattern observed for both peaks in the negative ion mode, which yielded the deprotonated molecules, and fragments at *m/z* 353 due to the loss of the *p*-coumaroyl moiety (85-95% RA) (Fig. 2S in the supplementary material) and at *m/z* 337 due to the loss of the caffeoyl moiety (40-50% RA) (Fig. 3S in the supplementary material) in the low energy function, indicating that the former loss was favored. This fragmentation pattern was reported for 3-*p*-coumaroyl-4-caffeoylquinic acid (3-*p*Co-4-CQA) and 4-caffeoyl-5-*p*-coumaroylquinic acid (4-C-5-*p*CoQA) (Clifford, Marks, Knight, & Kuhnert, 2006). The deprotonated quinic acid ion at *m/z* 191 was the base peak in the high energy function; this fragment is a characteristic base peak of 5-CQA, 3-CQA and 5-*p*CoQA, and is yielded by 4-CQA (Clifford et al., 2003). Thus, taking also into account that the elution order on endcapped C18 packing is 3,4-isomers, 3,5-isomers and 4,5-isomers (Clifford, Marks, et al., 2006), compounds **18** and **19** were tentatively assigned to 3-*p*Co-4-CQA and 4-C-5-*p*CoQA respectively, for the first time in lettuce cultivars. *p*-Coumaroylcaffeoylquinic acids have been previously reported in lettuce (Abu-Reidah et al., 2013; Jaiswal et al., 2011).

3.1.1.8. Dicaffeoyltartaric acids

Two peaks (**20**, **21**), presenting the same UV spectra as caffeic acid standard, were detected in the chromatograms extracted from the TIC MS scan chromatogram in positive and negative modes at *m/z* 475 and 473, respectively, which were due to two dicaffeoyltartaric acid isomers (diCTA). Compound **20** (Rt= 10.53 min, λmax= 301, 324 nm) and compound **21** (Rt= 12.54 min, λmax= 301, 323 nm) presented the same fragmentation pattern, and their identity was confirmed with the sodium adduct at *m/z* 497 in positive ionization mode and the $[2M-H]^-$ ion at *m/z* 947 in

negative mode for peak **20**, and the protonated and deprotonated molecules for peak **21**. In the negative ion mode, both peaks (**20**, **21**) yielded the same base peak at *m/z* 293 due to the loss of water of the deprotonated caffeoyltartaric acid, and $[CTA–H]^-$ at *m/z* 311 due to the loss of one of the caffeoyl moieties (Fig. 3S in the supplementary material), as well as ions from the tartaric moiety, $[\text{tartaric acid–H}]^-$ at *m/z* 149 and $[\text{tartaric acid–H–CO}_2]^-$ at *m/z* 105; and ions from the caffeoyl moiety, $[\text{caffeic acid–H}]^-$ at *m/z* 179 and $[\text{caffeic acid–H–CO}_2]^-$ at *m/z* 135. Compound **20** was tentatively identified as di-*O*-caffeoyltartaric (chicoric acid), and compound **21** as meso-di-*O*-caffeoyltartaric acid, since they were detected in lettuce elsewhere; the former being reported as the most abundant as we observed (Abu-Reidah et al., 2013; Jeong et al., 2015; Lin et al., 2012; Mai & Glomb, 2013; Pepe et al., 2015; Ribas-Agustí et al., 2011; Romani et al., 2002; Santos et al., 2014).

3.1.1.9. Other hydroxycinnamic acid derivatives

Several cinnamoyl glycosides were found in the lettuce extracts, such as caffeoyl-hexosides, *p*-coumaroyl-hexosides, sinapoyl-hexosides and dihydrocaffeic acid-hexosides, whose fragmentation patterns were characterized by the aglycone product ion resulted from the loss of a hexose residue (Abu-Reidah et al., 2013; Gómez-Romero, María, Zurek, Schneider, Baessmann, Segura-Carretero, & Fernández-Gutiérrez, 2011).

Eight peaks (**22**, Rt= 5.39 min; **23**, Rt= 5.64 min; **24**, Rt= 6.08 min, λmax= 301, 325 nm; **25**, Rt= 7.69 min; **26**, Rt= 8.44 min; **27**, Rt= 9.01 min; **28** Rt= 9.52 min; and **29** Rt= 9.64 min) were observed in the chromatogram extracted at *m/z* 343 and 341 in positive and negative ion modes respectively (Fig. 2S in the supplementary material). All of them (**22**-**29**) produced *m/z* 179 and 135 in negative ion mode, and *m/z* 163, 145, 135, 117 and 89 in positive ion mode, consistent with the presence of a caffeic acid residue. Thus, these compounds were tentatively assigned as isomeric caffeic acid-hexosides, in agreement with Clifford et al. (2007) (Clifford et al., 2007). Moreover, the identity of peaks **22**-**26** and **28** were confirmed by the presence of their sodium adducts in the positive low energy function. As well, peak **30** (Rt= 8.01 min, λmax= 301, 325 nm) showed the same fragmentation pattern as caffeic acid, yielding also a monoisotopic protonated molecule at

m/z 359.0802 ($C_{18}H_{15}O_8$) in the positive ion mode, and a monoisotopic deprotonated molecule at *m/z* 357.0633 ($C_{18}H_{13}O_8$) in the negative ion mode. Thus, it was tentatively assigned as a caffeoyl derivative, however the nature of the non-phenolic residue (196.0387 *u*) was not able to be disclosed. Such caffeoyl derivative has not previously been reported in lettuce so far we are aware.

Similarly, four isomers of synapic acid-hexosides (**31**, Rt= 6.03 min, λmax= 301, 326 nm; **32**, Rt= 9.70 min; **33**, Rt= 10.36 min; **34**, Rt= 13.13 min) were tentatively identified in the extracted traces at *m/z* 387 and 385 in the positive and the negative ion modes respectively (Fig. 2S in the supplementary material). Ions corresponding to the deprotonated aglycone at *m/z* 223, and the subsequent decarboxylations and losses of methyl residues at *m/z* 208, 179, 164, and 149 from the synapoyl moiety were detected in the negative ion mode. In addition, the positive ion mode yielded the sodium adduct at *m/z* 409 and ions due to the loss of the hexose residue at *m/z* 225, and subsequent losses of H_2O at *m/z* 207, CH_3OH at *m/z* 192, and CO at *m/z* 129. One isomer of synapic acid-hexoside has been previously reported in green lettuce cultivars (Abu-Reidah et al., 2013).

Following this fragmentation patterns, a *p*-coumaric acid-hexoside (**35**, Rt= 8.32 min) and two dihydrocaffeic acid-hexosides (**36**, Rt= 3.70 min; **37**, Rt= 3.83 min) were also characterized. All of them yielded the product ion due to the loss of the hexose residue (*m/z* 163 for **35**, *m/z* 181 for **36** and **37**), with the subsequent losses of H_2O, CO and CO_2 in the negative ion mode; and the sodium adduct in the positive ion mode (*m/z* 349 for **35**, *m/z* 367 for **36** and **37**).

Seven caffeic acid-hexosides, a synapic acid-hexosides, a dihydrocaffeic acid-hexoside and a *p*-coumaric acid-hexoside have been previously reported in green lettuce cultivars (Abu-Reidah et al., 2013). In the present work, one more caffeic acid-hexoside, a dihydrocaffeic acid-hexoside and three synapic acid-hexosides were identified in the butterhead lettuce cultivar.

Peaks **38** (Rt= 11.81 min, λmax= 307 nm), **39** (Rt= 14.47 min) and **40** (Rt= 16.48 min) were tentatively proposed as isomers of ferulic acid methyl esters. According to previous data (Abu-Reidah et al., 2013; Gómez-Romero, María et al., 2011), these compounds showed demethylated fragment ions at *m/z* 192 ($[M–H–CH_3]^-$) and *m/z* 177 ($[M–H–2CH_3]^-$), which is characteristic of the

methoxylated cinnamic acids. Two of these isomers of ferulic acid methyl esters have been previously reported in green lettuce cultivars.

3.1.2. Hydroxybenzoic derivatives

Hydroxybenzoic derivatives were not detected in the positive ion mode. Thus, no peaks were detected in the chromatograms extracted from the TIC MS scan chromatogram at the protonated molecule or the sodium adduct masses of the hydroxybenzoic derivatives observed in the negative ion mode. Only one of the two previously reported in green lettuce cultivars (Abu-Reidah et al., 2013) isomers of hydroxybenzoic acid (**41**: Rt= 4.67 min) and dihydroxybenzoic acid (**42**: Rt= 5.42 min) were detected at *m/z* 137 and *m/z* 153 respectively (Fig. 2S in the supplementary material). Their corresponding decarboxylated ions were also observed at *m/z* 93 and *m/z* 109 respectively.

Several hydroxybenzoic glycoside esters were characterized according to their MS data and fragmentation pattern by the neutral loss of the glycosidic moiety. Hydroxybenzoic acid-hexosides (**43**, Rt= 4.22 min; **44**, Rt= 5.15 min) yielded the deprotonated ion at *m/z* 299 and the product ions due to losses of the hexose residue (*m/z* 137) and CO_2 (*m/z* 93). Dihydroxybenzoic acid-hexosides (**45**, Rt= 2.49 min; **46**, Rt= 2.69 min; **47**, Rt= 3.74 min; **48**, Rt= 3.91 min; **49**, Rt= 4.48 min; **50**, Rt= 4.68 min) produced the deprotonated molecule at *m/z* 315 (base peak), an odd electron product ion at *m/z* 152 corresponding to the loss of hexose plus H (163 *u*), an even electron ion at *m/z* 153 due to the loss of hexose (Fig. 2S in the supplementary material), the dehydrated ion at *m/z* 135, and the decarboxylated ion at *m/z* 109, in agreement with bibliography (Abu-Reidah et al., 2013). Hence, one more hydroxybenzoic acid-hexoside and four more dihydroxybenzoic acid-hexosides are here detected in butterhead lettuce than in previous studies on different lettuce cultivars. The release of such unusual losses was also observed for gallic acid-hexoside isomers. Thus, peaks **51 (**Rt=2.80 min), **52 (**Rt=2.88 min) and **53 (**Rt=6.61 min) were tentatively proposed as gallic acid-hexosides, since they yielded the deprotonated molecule at *m/z* 331 (base peak) (Fig. 3S in the supplementary material), and an odd electron product ion at *m/z* 168, corresponding to the loss of hexose plus H (163 *u*), an even electron ion at *m/z* 169 due to the loss of hexose, and [gallic acid–H–CO_2]$^-$ at *m/z*

125. Two isomers of gallic acid-hexoside have been detected previously only in the lettuce cv. baby (Abu-Reidah et al., 2013).

Aside from the loss of the hexose moiety, syringic acid-hexoside (**54**, Rt= 5.90 min, *m/z* 359) showed subsequent losses of CH_3 from the methoxy groups of the aglycone and CO_2 (*m/z* 182, 153, 138 and 123), as previously observed in literature (Abu-Reidah et al., 2013; Gómez-Romero, María et al., 2011).

In agreement with previous studies (Abu-Reidah et al., 2013), compounds **55** (Rt= 17.09 min) and **56** (Rt= 24.83 min) showing a deprotonated molecule at *m/z* 451 were tentatively assigned as hydroxybenzoyl-gallic acid-hexosides (Fig. 3S in the supplementary material). The high energy function yielded the fragment ion corresponding to the deprotonated gallic acid-hexoside at *m/z* 331, after the loss of the hydroxybenzoyl moiety (120 *u*). As well, product ions due to successive losses of H_2O at *m/z* 313, hexose plus H at *m/z* 168 and CO_2 at *m/z* 124 were observed. A similar pattern was found for the hydroxybenzoyl-dihydroxybenzoic acid-hexosides (**57**, Rt= 17.68 min; **58**, Rt= 19.41 min; **59**, Rt= 23.64 min; **60**, Rt= 26.88 min, λmax= 256, 335 nm; **61**, Rt= 27.09 min) detected in the extracted trace at *m/z* 435 (Fig. 3S in the supplementary material). For peak **59**, only the deprotonated molecule was detected due to its low concentration in the extract. All other isomers yielded the fragment ions corresponding to [dihydroxybenzoic acid-hexoside–H]$^-$ at *m/z* 315, and the subsequent losses of H_2O at *m/z* 297 and hexose plus H at *m/z* 152 and CO_2 at *m/z* 108. Peaks **58** and **61** showed the product ion [dihydroxybenzoic acid–H]$^-$ due to an even electron ion at *m/z* 153 (loss of hexose), instead of the odd electron product ion at *m/z* 152. Besides, peaks **57**, **60** and **61**, yielded the fragment ion [hydroxybenzoic acid–H]$^-$ at *m/z* 137 and its corresponding decarboxylation ion at *m/z* 93. This behaviour agrees with that observed for hydroxycinnamic acid glycosides above and in literature (Clifford et al., 2007), which suggest that both, the hydroxybenzoic acid moiety and the dihydroxybenzoic acid moiety, are attached through their phenolic hydroxyl to different positions of the same hexose molecule. Just one isomer of

485 hydroxybenzoyl-gallic acid-hexoside and two isomers of hydroxybenzoyl-dihydroxybenzoic acid-
486 hexosides have been previously characterized only in cv. baby lettuce (Abu-Reidah et al., 2013).

487 **3.1.3. Hydroxyphenylacetic derivatives**

488 Taking into account the MS data, the fragmentation patterns observed for hydroxybenzoic
489 acid in the negative ion mode and bibliography (Abu-Reidah et al., 2013; Gómez-Romero, María et
490 al., 2011), 4-hydroxyphenylacetic acid was tentatively assigned to peak **62** (Rt= 5.60 min) (Fig. 4S
491 in the supplementary material), which yielded the deprotonated molecule at *m/z* 151 and fragment
492 ions due to the loss of CO at *m/z* 123 and CO_2 at *m/z* 107, showing the typical decarboxylation of
493 phenolic acids. Likewise, peak **63** (Rt= 5.20 min, λmax= 270, 276 nm) observed in the extracted
494 trace at *m/z* 313, produced the same decarboxylation ions, and a fragment ion at *m/z* 151 due to
495 deprotonated 4-hydroxyphenylacetic acid obtained after the loss of a hexose moiety (Fig. 4S in the
496 supplementary material). Thus, it was proposed as 4-hydroxyphenylacetic acid-hexoside. Both
497 compounds have been previously detected in green lettuce cultivars (Abu-Reidah et al., 2013).

498 **3.2. Flavonoids**

499 **3.2.1. Flavonols**

500 Thirteen quercetin glycosides (**64**-**76**) and four kaempferol glycosides (**77**-**80**) were detected
501 and identified on the basis of their mass spectral data, comparison with available standards, and
502 literature. Flavonol monoglycoside mass spectra in the positive mode showed the protonated
503 molecule $[M+H]^+$, the sodium adduct ion $[M+Na]^+$ and the protonated aglycone ion $[Y_0]^+$ as a result
504 of the loss of the sugar or organic acid residue (losses: 146 *u*, rhamnosyl residue; 162 *u*, hexosyl
505 residue; 176 *u*, glucuronic residue; 178 *u*, gluconic residue; 248 *u*, malonyl-hexosyl residue; 324 *u*,
506 di-hexosyl residue; 338 *u*, glucuronic + hexosyl residue; 410 *u*, hexosyl + malonyl-hexosyl residue;
507 424 *u*, glucuronic + malonyl-hexosyl residue). In the mass spectrum of flavonol diglycosides, a
508 fragment $[Y_1]^+$ due to the loss of the first sugar or organic acid unit was also observed. In the
509 negative mode, the high energy function product ions corresponding to quercetin at *m/z* 300 (odd
510 electron ion) and/or 301 (even electron ion) were detected (Fig. 4S in the supplementary material),

as observed in MS/MS elsewhere (Abu-Reidah et al., 2013). Regarding this, compounds **64** (Rt= 17.16 min, λmax= 279, 344 nm), **65** (Rt= 18.03 min, λmax= 252, 367 nm) and **66** (Rt= 20.25 min, λmax= 252, 330 nm) were identified as quercetin-3-*O*-hexosides on the basis of their protonated molecule at *m/z* 465 and a high energy function product ion at *m/z* 303, which indicates cleavage of a hexosyl group. This fragmentation pattern and chromatographic retention time of the reference standard confirmed that compound **66** was quercetin-3-*O*-galactoside. Two isomers of quercetin hexose have been previously described in lettuce (Abu-Reidah et al., 2013; Becker, Klaering, Schreiner, Kroh, & Krumbein, 2014; Jeong et al., 2015; Lin et al., 2012; Llorach et al., 2008; Mai & Glomb, 2013; Marin et al., 2015; Pepe et al., 2015; Romani et al., 2002; Santos et al., 2014; Sofo, Lundegårdh, Mårtensson, Manfra, Pepe, Sommella et al., 2016).

Compound **67** (Rt= 18.44 min, λmax= 254, 349 nm) was identified as quercetin-3-*O*-glucuronide because of $[M+H]^+$ at *m/z* 479, $[M+Na]^+$ at *m/z* 501 and $[Y_0]^+$ at *m/z* 303, which indicated the loss of a glucuronic residue in the positive mode (Fig. 2). Similarly, in the negative mode, the molecule $[M-H]^-$ at *m/z* 477 yielded $[Y_0]^-$ at *m/z* 301; the loss of 176 *u* pointed out the presence of a glucuronic residue (Fig. 2). The presence of quercetin-3-*O*-glucuronide in lettuce had been previously confirmed by nuclear magnetic resonance analysis (DuPont, Mondin, Williamson, & Price, 2000; Mai & Glomb, 2013). The glucuronic group was also observed in compound **68** (Rt= 9.50 min, λmax= 256, 352 nm) and compound **69** (Rt= 10.58 min), which gave $[M+H]^+$ at *m/z* 641, $[M+Na]^+$ at *m/z* 663, and $[Y_0]^+$ at *m/z* 303 in positive mode, and peak **69**, also $[Y_1]^+$ at *m/z* 465. In the negative mode, both compounds presented similar ionization and fragmentation pattern: $[M-H]^-$ at *m/z* 639, $[Y_1]^-$ at *m/z* 463 and $[Y_0]^-$ at *m/z* 300 (odd electron ion) and/or 301 (even electron ion). Moreover, the loss of 162 *u* revealed the cleavage of a hexoxyl group, therefore these flavonols were assigned to quercetin hexose-glucuronide isomers, which had been already described in baby, romaine and iceberg cultivars (Abu-Reidah et al., 2013).

Compounds **70** (Rt= 21.52 min, λmax= 255, 352 nm), **71** (Rt= 22.03 min, λmax= 252, 364 nm) and **72** (Rt= 23.69 min) were identified as quercetin malonylhexoside isomers since they

presented $[M+H]^+$ at *m/z* 551, $[M+Na]^+$ at *m/z* 573, and $[Y_0]^+$ at *m/z* 303 due to the loss of the malonylhexosyl moiety in the positive ion mode; and $[M-H]^-$at *m/z* 549, $[Y_0]^-$ at *m/z* 301 (Fig. 4S in the supplementary material), $[M-H-CO_2]^-$ at *m/z* 505 (base peak) in the negative ion mode. The neutral loss of CO_2 is characteristic of compounds presenting the malonyl group, as previously reported (Abu-Reidah et al., 2013). This fact is due to in-source fragmentation, which can affect the correct identification of the deprotonated molecule of interest, because the relative abundance of $[M-H]^-$ ion could be lower than the product ion $[M-H-CO_2]^-$ as occurred with these peaks. This particularly labile group could be partially lost during ion transfer from a higher-pressure region of the source to a lower-pressure region (Katta, Chowdhury, & Chait, 1991), as observed for peak **70** (0.4 % RA), peak **71** (11 % RA) and peak **72** (0.4 % RA). The identification of compound **70** was also confirmed by the presence of $[2M-H]^-$ ion. Quercetin-3-*O*-(6''-*O*-malonyl)-glucoside has been reported in lettuce in several publications (Becker et al., 2014; DuPont et al., 2000; Ferreres, Gil, Castañer, & Tomás-Barberán, 1997; Heimler, Isolani, Vignolini, Tombelli, & Romani, 2007; Llorach et al., 2008; Mai & Glomb, 2013; Marin et al., 2015; Ribas-Agustí et al., 2011; Romani et al., 2002; Santos et al., 2014), and confirmed by NMR analysis (DuPont et al., 2000; Ferreres et al., 1997). Two isomers of quercetin malonylglucoside were already described in different lettuce varieties (Abu-Reidah et al., 2013; Lin et al., 2012). The presence of three quercetin malonylhexoside isomers in lettuce is described for the first time in the present study.

Compound **73** (Rt= 11.51 min, λmax= 253, 355 nm) was identified as quercetin-3-*O*-(6"-*O*-malonyl)-glucoside-7-*O*-glucuronide, which has been previously described in lettuce (Abu-Reidah et al., 2013; Llorach et al., 2008; Santos et al., 2014). In the positive ion mode, $[M+H]^+$ at *m/z* 727, $[M+Na]^+$ at *m/z* 749, and the fragment ions $[Y_1]^+$ at *m/z* 479 and $[Y_0]^+$ at *m/z* 303 indicated the loss of a malonyl-glucosyl group followed by a glucuronic group. In the negative ion mode, the neutral loss of CO_2 yielding $[M-H-CO_2]^-$ at *m/z* 681 confirmed the presence of a malonyl residue in the molecular structure; as well as the high energy function product ions at *m/z* 300 (odd electron ion) and/or 301 (even electron ion) (Fig. 4S in the supplementary material), the presence of quercetin.

Similarly, compound **74** (Rt= 13.82 min, λmax= 253, 350 nm) also contained a malonyl residue since its base peak in the negative mode was $[M-H-CO_2]^-$ at *m/z* 667. The deprotonated molecule at *m/z* 711 was also present and $[Y_0]^-$ at *m/z* 300 (odd electron ion) and/or 301 (even electron ion) (Fig. 4S in the supplementary material) indicated that the aglycone was quercetin. The positive ion mode yielding $[M+H]^+$ at *m/z* 713, $[M+Na]^+$ at *m/z* 735, and the fragment ions $[Y_1]^+$ at *m/z* 465 and $[Y_0]^+$ at *m/z* 303 confirmed the cleavage of malonylhexosyl group followed by a hexosyl group. Thus, compound **74** was tentatively assigned to quercetin-3-*O*-(6"-*O*-malonyl)-glucoside-7-*O*-glucoside, which has been previously reported in lettuce (Abu-Reidah et al., 2013; Llorach et al., 2008; Santos et al., 2014), and confirmed by NMR analysis (Ferreres et al., 1997).

Compounds **75** (Rt= 12.18 min) and **76** (Rt= 16.07 min) presented the same monoisotopic molecular mass for $[M+H]^+$ at *m/z* 627.1580 ($C_{27}H_{31}O_{17}$) and $[M-H]^-$at *m/z* 625.1405 ($C_{27}H_{29}O_{17}$), and $[M+Na]^+$ at *m/z* 649.1381 ($C_{27}H_{30}O_{17}Na$). The presence of $[Y_0]^+$ at *m/z* 303 and $[Y_0]^-$ at *m/z* 301 (Fig. 4S in the supplementary material) in the positive and negative ion modes, respectively, disclosed that the aglycone was quercetin. However, these compounds followed different fragmentation patterns. Peak **75** yielded $[Y_1]^-$ at *m/z* 463 due to the loss of a hexosyl moiety (162 *u*), and revealing that $[Y_0]^-$ was obtained from the loss of a second hexosyl residue. Thus, compound **75** was assigned as a quercertin-*O*-di-hexoside. Instead, peak **76** yielded $[Y_1]^-$ at *m/z* 447 due to the loss of a gluconic moiety (178 *u*), and disclosing a subsequent loss of a rhamnosyl moiety (146 *u*) to achieve $[Y_0]^-$. Peak **75** was tentatively identified as quercetin-di-glucoside, which has been previously reported in green lettuce (Santos et al., 2014). Peak **76** was tentatively proposed as quercertin-*O*-rhamnosyl-gluconide, which is here reported for the first time to the author's knowledge.

Regarding kaempferol conjugates, compound **77** (Rt= 25.27 min, λmax= 265, 347 nm) was identified as kaempferol-3-*O*-(6''-*O*-malonyl)-glucoside, which has been already found in different lettuce cultivars (Heimler et al., 2007). In the positive mode, $[M+H]^+$ at *m/z* 535, $[M+Na]^+$ at *m/z* 557, and the fragment ions and $[Y_0]^+$ at *m/z* 287 revealed the cleavage of a malonyl-glucosyl group.

In the negative mode, $[M-H]^-$at *m/z* 533, $[Y_0]^-$ at *m/z* 285, $[M-H-CO_2]^-$ at *m/z* 489 confirmed the presence of the malonyl glucosyl moiety in the molecule (Fig. 4S in the supplementary material). Regarding the aglycone, kaempferol and the flavone luteolin are isobaric, but their conjugates can be distinguished on the basis of their MS and MS/MS data. In the positive low energy function, kaempferol derivatives yield $[Y_0]^+$ as the base peak or $[M+H]^+$ as the base peak plus an intense $[Y_0]^+$, whereas luteolin derivatives give as the base peak $[M+H]^+$ or $[M+H-H_2O]^+$, and $[Y_0]^+$ does not appear or present low relative abundance. In the negative low energy function, both compounds yield $[M-H]^-$ or $[M-H-CO_2]^-$ (in the case of malonylglycosides) as the base peak, but in the negative high energy function, kaempferol conjugates give the base peak $[Y_0]^-$, whereas luteolin compounds yield the base peak $[M-H]^-$ or $[M-H-CO_2]^-$ and an intense $[Y_0]^-$, or $[Y_0]^-$ as the base peak and an intense $[M-H]^-$ with relative abundance higher than 50% RA. Moreover, several minor monoisotopic product ions at *m/z* 217.0501 ($C_{12}H_9O_4$), 199.0395 ($C_{12}H_7O_3$), 175.0395 ($C_{10}H_7O_3$) and 133.0290 ($C_8H_5O_2$) are characteristic of luteolin, and helps to distinguish it from its kaempferol isomers (Abu-Reidah et al., 2013; Gómez-Romero, María et al., 2011). In this sense, these fragment ions did not appear in the negative high energy MS spectra of peak **77**, suggesting that it is a kaempferol derivative. Moreover, this identification was also supported by the base peaks yielded in the positive low energy and the negative high energy functions, $[Y_0]^+$ and $[Y_0]^-$ respectively, as well as its UV-visible spectra, and elution order since kaempferol isomers elute later than luteolin isomers on endcapped C_{18} packings.

Two isomers (**78**: Rt= 23.90 min; **79**: Rt= 26.43 min) were detected in the extracted MS chromatogram at *m/z* 449 and 447 in the positive and negative ion modes respectively, which yielded the protonated ion, $[M+Na]^+$ at *m/z* 471 and $[Y_0]^+$ at *m/z* 287 in the positive ion mode, and the deprotonated molecule and $[Y_0]^-$ at *m/z* 285 in the negative ion mode (Fig. 4S in the supplementary material); revealing the loss of a hexosyl residue and the presence of kaempferol or luteolin aglycone. The base peaks yielded in the positive low energy and the negative high energy functions were $[Y_0]^+$ and $[Y_0]^-$ respectively, and no characteristic minor product ions of luteolin

were detected in the negative high energy function, therefore the aglycone was tentatively identified as kaempferol. Compound **78** was identified unambiguously as kaempferol-3-*O*-glucoside by comparison with its standard, whereas compound **79** as kaempferol-hexoside. Kaempferol-3-*O*-glucoside is the only kaempferol-hexoside that has been previously detected in several lettuce cultivars (Alarcón-Flores et al., 2016).

Compound **80** (Rt= 22.34 min, λmax= 265, 332 nm) was identified as kaempferol-3-*O*-glucuronide, which has been previously found in lettuce in literature (Jeong et al., 2015). This compound yielded $[M+H]^+$ at *m/z* 463, $[M+Na]^+$ at *m/z* 485 and $[Y_0]^+$ at *m/z* 287 in the positive mode; and $[M-H]^-$ at *m/z* 461 and $[Y_0]^-$ at *m/z* 285 in the negative mode (Fig. 4S in the supplementary material). The observed loss of 176 *u* pointed out the presence of a glucuronic residue. Besides, the presence of the base peaks $[Y_0]^+$ and $[Y_0]^-$ in the positive low energy and the negative high energy functions respectively, and the absence of luteolin characteristic minor product ions in the negative high energy function, supports the proposed identification for this compound.

Peak **81** (Rt= 27.08 min) presented the protonated and deprotonated molecules at *m/z* 287 and 285 in the positive and the negative ion modes respectively (Fig. 4S in the supplementary material), which yielded fragment ions characteristics of kaempferol or luteolin aglycones (Abad-García et al., 2009), suggesting that both compounds were eluting overlapped in this peak. To the author's knowledge, kaempferol aglycone has not been previously found in lettuce, but in escarole (Asteraceae) (Llorach et al., 2008).

3.2.2. Flavones

Four luteolin glycosides (**82-85**) and four apigenin conjugates (**86-89**) were detected and identified on the basis of mass spectral data, comparing with available standards and bibliographic sources. Compound **82** (Rt= 19.82 min, λmax= 255, 347 nm) was identified unambiguously as luteolin-7-*O*-glucoside by comparison with its standard, which showed the deprotonated molecule at *m/z* 447, $[2M-H]^-$ at *m/z* 895, $[Y_0]^-$ at *m/z* 285 (Fig. 4S in the supplementary material), and

luteolin characteristic minor product ions at *m/z* 217, 199 and 175 in the negative ion mode; and the protonated molecule at *m/z* 449, $[M+Na]^+$ at *m/z* 471, $[Y_0]^+$ at *m/z* 287, and intense fragment ions at 153 and 135 in the positive mode. Luteolin-7-*O*-glucoside has been previously described in lettuce cultivars (Abu-Reidah et al., 2013; Alarcón-Flores et al., 2016; Lin et al., 2012).

Compound **83** (Rt= 17.45 min, λmax= 253, 348 nm) was assigned to luteolin-7-*O*-glucuronide regarding the protonated molecule yielded at *m/z* 463, $[M+Na]^+$ at *m/z* 485 and $[Y_0]^+$ at *m/z* 287, which revealed the cleavage of a glucuronic residue. In the negative high energy function, compound **83** yielded the corresponding deprotonated molecule at *m/z* 461, $[Y_0]^-$ at *m/z* 285 , as well as some minor fragment ions at *m/z* 217, 199, 175, 151 and 133 (Fig. 4S and 7S in the supplementary material), which distinguished luteolin conjugates from its kaempferol isomers (Abu-Reidah et al., 2013; Gómez-Romero, María et al., 2011). This identification was supported by its UV-visible spectrum, which followed the luteolin pattern; and its elution order on encapped C18 packings, glucuronide conjugates elute earlier than their corresponding glucoside ones. Luteolin-7-*O*-glucuronide has been previously reported in lettuce (Abu-Reidah et al., 2013; DuPont et al., 2000; Lin et al., 2012; Mai & Glomb, 2013; Santos et al., 2014), and confirmed by NMR analysis (DuPont et al., 2000; Ferreres et al., 1997).

Compounds **84** (Rt= 20.27 min) and **85** (Rt= 21.17 min, λmax= 268, 351 nm) showed base peaks at *m/z* 595 ($[M+H]^+$) in the low energy function. Aside, compound **85** also presented the sodium adduct (*m/z* 617), the fragment ions at *m/z* 449 ($[Y_1]^+$), and at *m/z* 287 ($[Y_0]^+$) in the high energy function in the positive ion mode. This fragmentation pattern revealed the loss of rhamnosyl group followed by a hexosyl group, which is in agreement with the fragment ions observed in the negative ion mode, i.e. $[Y_1]^-$ at *m/z* 447 and $[Y_0]^-$ at *m/z* 285 (Fig. 4S in the supplementary material). In the negative ion mode, both compounds yielded the deprotronated molecule as the base peak in both low and high energy functions, supporting their tentatively assignment as luteolin-rhamnosylhexoside. Compound **85** was tentatively identified as luteolin-7-*O*-rutinoside since it was the major compound and has been previously found in different lettuce cultivars (Llorach et al.,

2008). The second luteolin-rhamnosylhexoside (**84**) is here reported for the first time in lettuce to the authors' knowledge.

Regarding apigenin derivatives, the observation of neutral losses of the conjugated groups and the product ions at *m/z* 271 and 269 in the positive and negative ion modes respectively, indicated the presence of apigenin in their structure (Fig. 4S in the supplementary material). Thus, compound **86** (Rt= 20.57 min) showing a loss of 176 *u* was identified as apigenin-glucuronide; compound **87** (Rt= 23.02 min, λmax= 259, 328 nm) with a loss of 162 *u*, as apigenin-glucoside; and compound **88** (Rt= 23.90 min) with subsequent losses of 146 *u* and 162 *u*, as apigenin-rhamnosylhexoside, which is here reported for the first time in lettuce cultivars. Likewise, compound **89** (Rt= 26.99 min) yielded the protonated and deprotonated molecules at *m/z* 839 and 837 and the corresponding apigenin aglycone ions in positive and negative ion modes respectively, showing a monoisotopic loss of 568.2731 *u* ($C_{25}H_{44}O_{14}$), however its identity was not able to be disclosed with the available spectral data. Apigenin-glucuronide (**86**) and apigenin-glucoside (**87**) have been already found in lettuce (Abu-Reidah et al., 2013; Alarcón-Flores et al., 2016). Alarcón-Flores et al. (2016) found an apigenin-*O*-derivative with the same fragmentation pattern as apigenin-rhamnosylhexoside (**88**) in different lettuce cultivars, as well as luteolin aglycone (**90**, Rt= 27.08 min). However, the apigenin conjugate (**89**) has not been previously reported.

3.2.3. Flavanones

A flavanone glycoside was detected and identified on the basis of its UV-visible spectrum and mass spectral data. Chromatographic peak **91** (Rt= 14.87 min, λmax= 284 nm, shoulder at 329 nm) in the negative mode yielded the base peaks $[M-H]^-$ at *m/z* 463 in the low energy function, and a fragment ion $[^{1,3}A]^-$ at *m/z* 151 and an intense ion $[Y_0]^-$ at *m/z* 287 (60% RA) in the high energy function (Fig. 3 and Fig. 5S in the supplementary material). In the positive ion mode, $[M+H]^+$ at *m/z* 465 (60% RA), $[M+Na]^+$ at *m/z* 487 and a fragment ion $[Y_0]^+$ at *m/z* 289 (base peak) were detected (Fig. 3). Both fragment ions revealed the cleavage of a glucuronic group. Moreover, a minor fragment $[^{1,3}A]^+$ at *m/z* 153 in the positive ion mode contributed to confirm that the aglycone was

eriodictyol (Abad-García et al., 2009). Thus, compound **91** was identified as eriodictyol-*O*-glucuronide, which is reported for the first time in lettuce to our best knowledge.

3.3. Coumarins

Seven coumarins (**92-98**) were detected in butterhead lettuce cultivar. Chromatographic peak **92** (Rt= 6.50 min, λmax= 290, 340 nm) was identified as a 6,7-dihydroxycoumarin-6-*O*-glucoside (esculin) regarding its UV-visible spectrum and mass spectral data. In the positive ion mode, the protonated molecule at *m/z* 341, the sodium adduct at *m/z* 363 and $[Y_0]^+$ at *m/z* 179 were produced, indicating that a hexosyl group was present in the molecular structure. This was confirmed in the negative ion mode, where the deprotonated molecular at *m/z* 339, the acetate adduct $[M-H+AcO]^-$ at *m/z* 399 and $[Y_0]^-$ at *m/z* 177 were yielded (Fig. 5S in the supplementary material). Compound **92** also gave some minor fragment ions at *m/z* 133 and 105 corresponding to the loss of CO_2 and CO successively (Fig. 8S in the supplementary material), which have been previously reported in literature (Abu-Reidah et al., 2013), and suggested that peak **92** was esculetin-6-*O*-glucoside.

Compounds **93** (Rt= 7.31 min), **94** (Rt= 10.23 min) and **95** (Rt= 12.02 min, λmax= 296, 330 nm) presented the same protonated molecules at *m/z* 179 and deprotonated molecules at *m/z* 177 (Fig. 5S in the supplementary material), as well as the same fragmentation pattern described above for esculin. Thus, they were tentatively identified as dihydrocoumarin isomers. Esculin and 6,7-dihydrocoumarin (**95**) have been already reported in lettuce and Asteraceae (Abu-Reidah et al., 2013; Schütz, Carle, & Schieber, 2006). In the same way, compounds **96** (Rt= 9.05 min), **97** (Rt= 10.54 min) and **98** (Rt= 12.54 min) presented the same fragmentation patterns as the dihydrocoumarin isomers (Fig. 5S in the supplementary material), but their protonated molecules at *m/z* 295 and deprotonated molecules at *m/z* 293 disclosed that the loss to yield the dihydrocoumarin ion was 116 *u*, due to a maloyl residue. Thus, these compounds were tentatively assigned as maloyl-dihydrocoumarin isomers. Regarding the elution order of the dihydrocoumarin and the maloyl-dihydrocoumarin isomers, the latters are probably the maloyl derivatives of the formers, since the maloyl group increase the hydrophobicity of the molecule, and therefore, elute at higher retention

719 times in reverse-phase packings. To the authors' knowledge, maloyl-dihydrocoumarins are reported
720 in lettuce and Asteracea for the first time.

721 **3.4. Hydrolysable tannins**

722 A tri-4-hydroxyphenylacetyl ester of a hexose (**99**, Rt= 27.09 min) was detected in the
723 extracted trace at *m/z* 581 in the negative ion mode. This peak showed the characteristic
724 fragmentation pattern previously described in literature (Abu-Reidah et al., 2013), yielding
725 fragment ions at *m/z* 295 ([(4-hydroxyphenylacetic acid-hexose)−H−H_2O]$^-$), *m/z* 175 ([(4-
726 hydroxyphenylacetic acid-hexose)−2H−H_2O−$C_6H_5CH_2CO$]$^-$), *m/z* 151 ([4-hydroxyphenylacetic
727 acid−H]$^-$ (Fig. 4S in the supplementary material) and *m/z* 143 ([(4-hydroxyphenylacetic acid-
728 hexose)−2H−H_2O−$OHC_6H_4CH_2COOH$]$^-$ or [hexose−H−2H_2O]$^-$). Four isomers of tri-4-
729 hydroxyphenylacetyl-glucoside were found in several *Latuca* species (Abu-Reidah et al., 2013).

730 **3.5. Lignan derivatives**

731 Peak **100** (Rt= 21.00 min), detected in the extracted MS chromatogram set at *m/z* 417 in the
732 negative ion mode (Fig. 5S in the supplementary material), yielded the fragment ion *m/z* 359 due to
733 the losses of two methyl moieties plus CO. In the positive ion mode, the corresponding protonated
734 molecule was detected at *m/z* 419. This compound was tentatively identified as syringaresinol,
735 having not been found in lettuce cultivars before to the best of our knowledge. In relation to this
736 compound, four syringaresinol-hexoses (**101**, Rt= 13.90 min; **102**, Rt= 18.97 min; **103**, Rt= 19.63
737 min; **104**, Rt= 23.30 min) were detected in the extracted trace at *m/z* 579 and 581 in the negative
738 and positive ion modes. For peak **102**, only the corresponding deprotonated and protonated
739 molecules were detected due to its low concentration in the extract. All other isomers yielded in the
740 negative ion mode the fragment ions corresponding to the loss of the hexose residue (*m/z* 417) (Fig.
741 5S in the supplementary material), and the subsequent losses of H_2O (*m/z* 399) or two methyl
742 residues (*m/z* 387) from the syringaresinol. In the positive ion mode, the sodium adducts (*m/z* 603)
743 and the fragment ion due to the loss of the hexose residue plus two H_2O (*m/z* 383) were detected. In
744 addition, three isomers of syringaresinol-acetylhexoses (**105**, Rt= 15.06 min, λmax= 205, 280 nm;

745 **106**, Rt= 24.50 min; **107**, Rt= 24.63 min) were detected in the extracted trace at *m/z* 621 in the
746 negative ion mode, presenting the same aforementioned fragmentation pattern. In this sense, the
747 fragment ions due to the loss of the acetylhexose residue (*m/z* 417) (Fig. 5S in the supplementary
748 material), and the successive losses of H_2O (*m/z* 399), and methyl residues (*m/z* 402 ($-CH_3$), *m/z*
749 387 ($-2CH_3$)) and *m/z* 359 ($-2CH_3CO$)) were observed, as well as other further fragments from the
750 syringaresinol structure at *m/z* 181, 166, 151 and 123 (Fig. 9S in the supplementary material).
751 Peaks **108** (Rt= 19.22 min), **109** (Rt= 19.39 min) and **110** (Rt= 19.82 min) were observed in
752 the chromatogram set at *m/z* 581 in the negative ion mode (Fig. 5S in the supplementary material).
753 The MS spectra of these compounds disclosed that they presented the same fragmentation pattern as
754 the above lignans, yielding the product ions due to the loss of the dimethoxyhexose moiety (*m/z*
755 359), and the subsequent losses of H_2O (*m/z* 341), and two methyl residues (*m/z* 329) from the
756 lariciresinol structure. Thus, these compounds were proposed to be isomers of dimethoxy-hexosyl-
757 lariciresinol. Furthermore, a dimethoxy-dihexosyl-lariciresinol isomer (**111**: Rt= 16.37 min) was
758 also tentatively identified according to the presence of the deprotonated ion at *m/z* 743 and the
759 fragment ion due to the loss of a hexose residue at *m/z* 581 in its negative ion MS spectra, which
760 yielded further product ions following the same fragmentation pattern of dimethoxy-hexosyl-
761 lariciresinol. In lettuce cultivars, only one isomer of syringaresinol-hexose (syringaresinol-β-D-
762 glucoside) and dimethoxy-hexosyl-lariciresinol have been previously reported (Abu-Reidah et al.,
763 2013).
764 In conclusion, the UHPLC-DAD-ESI-QToF/MS^E approach demonstrates to be a useful tool
765 for the characterization of phenolic compounds in complex plant matrices.
766 **Acknowledgements**
767 The authors gratefully acknowledge the Agencia Nacional de Promoción Científica y
768 Tecnológica (project number PICT-2008-1724) and the Consejo Nacional de Investigaciones
769 Científicas y Técnicas (CONICET) (project number PIP 0007) from Argentina for the financial

support. Gabriela Elena Viacava thanks CONICET and Asociación Universitaria Iberoamericana de Postgrado (AUIP) for her Ph.D. grants.

References

Abad-García, B., Berrueta, L. A., Garmón-Lobato, S., Gallo, B., & Vicente, F. (2009). A general analytical strategy for the characterization of phenolic compounds in fruit juices by high-performance liquid chromatography with diode array detection coupled to electrospray ionization and triple quadrupole mass spectrometry. *Journal of Chromatography A, 1216*, 5398-5415.

Abu-Reidah, I. M., Contreras, M. M., Arráez-Román, D., Segura-Carretero, A., & Fernández-Gutiérrez, A. (2013). Reversed-phase ultra-high-performance liquid chromatography coupled to electrospray ionization-quadrupole-time-of-flight mass spectrometry as a powerful tool for metabolic profiling of vegetables: *Lactuca sativa* as an example of its application. *Journal of Chromatography A, 1313*, 212-227.

Agüero, M. V., Viacava, G. E., Ponce, A. G., & Roura, S. I. (2013). Early postharvest time period affects quality of butterhead lettuce packed in crates. *International Journal of Vegetable Science, 19*, 384-402.

Alarcón-Flores, M. I., Romero-González, R., Martínez Vidal, J. L., & Garrido Frenich, A. (2016). Multiclass determination of phenolic compounds in different varieties of tomato and lettuce by ultra high performance liquid chromatography coupled to tandem mass spectrometry. *International Journal of Food Properties, 19*, 494-507.

Alonso-Salces, R. M., Guillou, C., & Berrueta, L. A. (2009). Liquid chromatography coupled with ultraviolet absorbance detection, electrospray ionization, collision-induced dissociation and tandem mass spectrometry on a triple quadrupole for the on-line characterization of polyphenols and methylxanthines in green coffee beans. *Rapid Communications in Mass Spectrometry, 23*, 363-383.

795 Altunkaya, A., & Gökmen, V. (2009). Effect of various anti-browning agents on phenolic
796 compounds profile of fresh lettuce (L. sativa). *Food Chemistry, 117*, 122-126.
797 Becker, C., Klaering, H. P., Schreiner, M., Kroh, L. W., & Krumbein, A. (2014). Unlike quercetin
798 glycosides, cyanidin glycoside in red leaf lettuce responds more sensitively to increasing
799 low radiation intensity before than after head formation has started. *Journal of Agricultural*
800 *and Food Chemistry, 62*, 6911-6917.
801 Clifford, M. N., Johnston, K. L., Knight, S., & Kuhnert, N. (2003). Hierarchical scheme for LC-
802 MS^n identification of chlorogenic acids. *Journal of Agricultural and Food Chemistry, 51*,
803 2900-2911.
804 Clifford, M. N., Kirkpatrick, J., Kuhnert, N., Roozendaal, H., & Salgado, P. R. (2008). LC-MS^n
805 analysis of the cis isomers of chlorogenic acids. *Food Chemistry, 106*, 379-385.
806 Clifford, M. N., Knight, S., & Kuhnert, N. (2005). Discriminating between the six isomers of
807 dicaffeoylquinic acid by LC-MS^n. *Journal of Agricultural and Food Chemistry, 53*, 3821-
808 3832.
809 Clifford, M. N., Knight, S., Surucu, B., & Kuhnert, N. (2006). Characterization by LC-MS^n of four
810 new classes of chlorogenic acids in green coffee beans: Dimethoxycinnamoylquinic acids,
811 diferuloylquinic acids, caffeoyl-dimethoxycinnamoylquinic acids, and feruloyl-
812 dimethoxycinnamoylquinic acids. *Journal of Agricultural and Food Chemistry, 54*, 1957-
813 1969.
814 Clifford, M. N., Marks, S., Knight, S., & Kuhnert, N. (2006). Characterization by LC-MS^n of four
815 new classes of p-coumaric acid-containing diacyl chlorogenic acids in green coffee beans.
816 *Journal of Agricultural and Food Chemistry, 54*, 4095-4101.
817 Clifford, M. N., Wu, W., Kirkpatrick, J., & Kuhnert, N. (2007). Profiling the chlorogenic acids and
818 other caffeic acid derivatives of herbal chrysanthemum by LC-MS^n. *Journal of Agricultural*
819 *and Food Chemistry, 55*, 929-936.

820 Dai, J., & Mumper, R. J. (2010). Plant phenolics: extraction, analysis and their antioxidant and
821 anticancer properties. *Molecules, 15*, 7313-7352.
822 Dawidowicz, A. L., & Typek, R. (2011). The influence of pH on the thermal stability of 5-*O*-
823 caffeoylquinic acids in aqueous solutions. *European Food Research and Technology, 233*,
824 223-232.
825 DuPont, M. S., Mondin, Z., Williamson, G., & Price, K. R. (2000). Effect of variety, processing,
826 and storage on the flavonoid glycoside content and composition of lettuce endive. *Journal of*
827 *Agricultural and Food Chemistry, 48*, 3957-3964.
828 Ferreres, F., Gil, M. I., Castañer, M., & Tomás-Barberán, F. A. (1997). Phenolic Metabolites in Red
829 Pigmented Lettuce (Lactuca sativa). Changes with Minimal Processing and Cold Storage.
830 *Journal of Agricultural and Food Chemistry, 45*, 4249-4254.
831 Gómez-Romero, M., Segura-Carretero, A., & Fernandez-Gutierrez, A. (2010). Metabolite profiling
832 and quantification of phenolic compounds in methanol extracts of tomato fruit.
833 *Phytochemistry, 71*, 1848-1864.
834 Gómez-Romero, M., Zurek, G., Schneider, B., Baessmann, C., Segura-Carretero, A., & Fernández-
835 Gutiérrez, A. (2011). Automated identification of phenolics in plant-derived foods by using
836 library search approach. *Food Chemistry, 124*, 379-386.
837 Heimler, D., Isolani, L., Vignolini, P., Tombelli, S., & Romani, A. (2007). Polyphenol content and
838 antioxidative activity in some species of freshly consumed salads. *Journal of Agricultural*
839 *and Food Chemistry, 55*, 1724-1729.
840 Jaiswal, R., Kiprotich, J., & Kuhnert, N. (2011). Determination of the hydroxycinnamate profile of
841 12 members of the Asteraceae family. *Phytochemistry, 72*, 781-790.
842 Jeong, S. W., Kim, G.-S., Lee, W. S., Kim, Y.-H., Kang, N. J., Jin, J. S., Lee, G. M., Kim, S. T.,
843 Abd El-Aty, A. M., Shim, J.-H., & Shin, S. C. (2015). The effects of different night-time
844 temperatures and cultivation durations on the polyphenolic contents of lettuce: Application
845 of principal component analysis. *Journal of Advanced Research, 6*, 493-499.

Katta, V., Chowdhury, S. K., & Chait, B. T. (1991). Use of a single-quadrupole mass spectrometer for collision-induced dissociation studies of multiply charged peptide ions produced by electrospray ionization. *Analytical Chemistry, 63*, 174-178.

Lin, L. Z., Harnly, J., Zhang, R. W., Fan, X. E., & Chen, H. J. (2012). Quantitation of the hydroxycinnamic acid derivatives and the glycosides of flavonols and flavones by UV absorbance after identification by LC-MS. *Journal of Agricultural and Food Chemistry, 60*, 544-553.

Lozac'h, N. (1975). Nomenclature of Cyclitols. *European Journal of Biochemistry, 57*, 1-7.

Llorach, R., Martínez-Sánchez, A., Tomás-Barberán, F. A., Gil, M. I., & Ferreres, F. (2008). Characterisation of polyphenols and antioxidant properties of five lettuce varieties and escarole. *Food Chemistry, 108*, 1028-1038.

Ma, Y. L., Li, Q. M., Van den Heuvel, H., & Claeys, M. (1997). Characterization of flavone and flavonol aglycones by collision-induced dissociation tandem mass spectrometry. *Rapid Communications in Mass Spectrometry, 11*, 1357-1364.

Mai, F., & Glomb, M. A. (2013). Isolation of phenolic compounds from iceberg lettuce and impact on enzymatic browning. *Journal of Agricultural and Food Chemistry, 61*, 2868-2874.

Marin, A., Ferreres, F., Barberá, G. G., & Gil, M. I. (2015). Weather variability influences color and phenolic content of pigmented baby leaf lettuces throughout the season. *Journal of Agricultural and Food Chemistry, 63*, 1673-1681.

Markham, K. R. (1982). *Techniques of Flavonoid Identification*. London: AcademicPress Inc.

Pepe, G., Sommella, E., Manfra, M., De Nisco, M., Tenore, G. C., Scopa, A., Sofo, A., Marzocco, S., Adesso, S., Novellino, T., & Campiglia, P. (2015). Evaluation of anti-inflammatory activity and fast UHPLC-DAD-IT-TOF profiling of polyphenolic compounds extracted from green lettuce (*Lactuca sativa* L.; Var. Maravilla de Verano). *Food Chemistry, 167*, 153-161.

871 Ramirez-Ambrosi, M., Abad-Garcia, B., Viloria-Bernal, M., Garmon-Lobato, S., Berrueta, L. A., &
872 Gallo, B. (2013). A new ultrahigh performance liquid chromatography with diode array
873 detection coupled to electrospray ionization and quadrupole time-of-flight mass
874 spectrometry analytical strategy for fast analysis and improved characterization of phenolic
875 compounds in apple products. *Journal of Chromatography A, 1316*, 78-91.
876 Ribas-Agustí, A., Gratacós-Cubarsí, M., Sárraga, C., García-Regueiro, J. A., & Castellari, M.
877 (2011). Analysis of eleven phenolic compounds including novel p-coumaroyl derivatives in
878 lettuce (*Lactuca sativa* L.) by ultra-high-performance liquid chromatography with
879 photodiode array and mass spectrometry detection. *Phytochemical Analysis, 22*, 555-563.
880 Romani, A., Pinelli, P., Galardi, C., Sani, G., Cimato, A., & Heimler, D. (2002). Polyphenols in
881 greenhouse and open-air-grown lettuce. *Food Chemistry, 79*, 337-342.
882 Santos, J., Oliveira, M. B. P. P., Ibáñez, E., & Herrero, M. (2014). Phenolic profile evolution of
883 different ready-to-eat baby-leaf vegetables during storage. *Journal of Chromatography A,*
884 *1327*, 118-131.
885 Schütz, K., Carle, R., & Schieber, A. (2006). Taraxacum–A review on its phytochemical and
886 pharmacological profile. *Journal of Ethnopharmacology, 107*, 313-323.
887 Sobolev, A. P., Brosio, E., Gianferri, R., & Segre, A. L. (2005). Metabolic profile of lettuce leaves
888 by high-field NMR spectra. *Magnetic Resonance in Chemistry, 43*, 625-638.
889 Sofo, A., Lundegårdh, B., Mårtensson, A., Manfra, M., Pepe, G., Sommella, E., De Nisco, M.,
890 Tenore, G. C., Campiglia, P., & Scopa, A. (2016). Different agronomic and fertilization
891 systems affect polyphenolic profile, antioxidant capacity and mineral composition of lettuce.
892 *Scientia Horticulturae, 204*, 106-115.
893 Watson, R. R., Preedy, V. R., & Zibadi, S. (2014). *Polyphenols in human health and disease* (1st
894 ed.). San Diego: Academic Press.

895

Figure captions

Fig. 1. Chemical structures of phenolic compounds found in butterhead lettuce cultivar. Abbreviations for the phenolic moieties: C, caffeoyl; pCo, *p*-coumaroyl; F, feruloyl; dhC, dihydrocaffeoyl; Sp, sinapoyl; 4-OH-Bz, 4-hydroxybenzoyl; 3,4-diOH-Bz, 3,4-dihydroxybenzoyl; Gal, galloyl; Syr, syringoyl; 4-OH-PhAc, 4-hydroxyphenylacetoyl; Que, quercetin (Z_1=OH, Z_2=OH); Kaemp, kaempferol (Z_1=H, Z_2=OH); Lut, luteolin (Z_1=OH, Z_2=H); Api, apigenin (Z_1=H, Z_2=H); 6,7-diOH-Cou, 6,7-dihidroxycoumarin. Abbreviations for the non-phenolic moieties: Q, quinic acid; Tar, tartaric acid, Mal, malic acid; Mln, malonic acid; Glcr, glucuronic acid; Glcn, gluconic acid; Hex, hexose; Rha, rhamnose; Rut, rutinose (rhamnosylglucose). R, R_1, R_2, R_3, R_4 and R_5 in non-phenolic moieties can be esterified in position X of phenolic acids or etherified with phenolic OH groups.

Fig. 2. Low (F1) and high (F2) energy function MS spectra in the negative and positive ion mode of quercetin-3-*O*-glucuronide. ESI, electrospray ionization.

Fig. 3. Low (F1) and high (F2) energy function MS spectra in the negative and positive ion mode of eriodictyol-*O*-glucuronide. ESI, electrospray ionization.

Supplementary material

Fig. 1S. Low energy function (F1) base peak chromatograms in positive and negative ion modes and DAD chromatograms at 280 and 370 nm of the butterhead lettuce cultivar.

Fig. 2S. Butterhead lettuce cultivar chromatograms extracted from the TIC-MS scan chromatogram in negative ion mode at *m/z* 353, 341, 385 and 153 of the low energy function (F1). Chromatographic peaks are numbered as in Tables 1.

Fig. 3S. Butterhead lettuce cultivar chromatograms extracted from the TIC-MS scan chromatogram in negative ion mode at *m/z* 337, 311, 331, 451 and 435 of the low energy function (F1). Chromatographic peaks are numbered as in Tables 1.

Fig. 4S. Butterhead lettuce cultivar chromatograms extracted from the TIC-MS scan chromatogram in negative ion mode at *m/z* 151 of the low energy function (F1), and at *m/z* 301, 285 and 269 of the high energy function (F2). Chromatographic peaks are numbered as in Tables 1.

Fig. 5S. Butterhead lettuce cultivar chromatograms extracted from the TIC-MS scan chromatogram in negative ion mode at *m/z* 287, 177 and 581 of the low energy function (F1), and at *m/z* 417 of the high energy function (F2). Chromatographic peaks are numbered as in Tables 1.

Fig. 6S. Low (F1) and high (F2) energy function MS spectra in the negative and positive ion mode of 5-*trans*-*O*-caffoylquinic acid. ESI, electrospray ionization.

Fig. 7S. Low (F1) and high (F2) energy function MS spectra in the negative and positive ion mode of luteolin-7-*O*-glucuronide. ESI, electrospray ionization.

Fig. 8S. Low (F1) and high (F2) energy function MS spectra in the negative and positive ion mode of esculetin-6-*O*-glucoside. ESI, electrospray ionization.

Fig. 9S. Low (F1) and high (F2) energy function MS spectra in the negative and positive ion mode of syringaresinol-acetylhexose. ESI, electrospray ionization.

Table 1

Retention times, UV-visible maxima and MS^{E} data of polyphenols identified by UHPLC-DAD-ESI-Q-ToF/MS in the butterhead lettuce cultivar.[a, b, c]

	LC	DAD	ESI(+)–QToF/MS					ESI(–)–QToF/MS					Assignment
Nº	**Rt (min)**	**UV bands (nm)**	**Exp. Acc. Mass $[M+H]^+$**	**Error (mDa)**	**Formula $[M+H]^+$**	**Adducts & fragment ions of $[M+H]^+$** *m/z*		**Exp. Acc. Mass $[M-H]^-$**	**Error (mDa)**	**Formula $[M-H]^-$**	**Adducts & fragment ions of $[M-H]^-$** *m/z*		**Tentative identification**
Phenolic acids													
Hydroxycinnamic derivatives													
Caffeoylquinic acids													
1	4.74	301 sh, 323	355.1068	3.9	$C_{16}H_{19}O_9$	377.0858	$[M+Na]^+$	353.0872	–0.1	$C_{16}H_{17}O_9$	191.0556	$[Quin-H]^-$ *(100)*	3–*trans*–*O*–Caffeoylquinic acid
						163.0398	$[Caffeoyl+H]^+$				179.0348	$[Caffeic-H]^-$ *(32)*	
						145.0279	$[Caffeoyl+H-H_2O]^+$				173.0437	$[Quin-H-H_2O]^-$ *(4)*	
						135.0448	$[Caffeoyl+H-CO]^+$				135.0446	$[Caffeic-H-CO_2]^-$ *(71)*	
						117.0343	$[Caffeoyl+H-CO-H_2O]^+$						
						89.0397	$[Caffeoyl+H-H_2O-2CO]^+$						
2	6.65	-	355.1026	–0.3	$C_{16}H_{19}O_9$	731.1791	$[2M+Na]^+$	353.0869	0.4	$C_{16}H_{17}O_9$	707.1821	$[2M-H]^-$	1–*trans*–*O*–Caffeoylquinic acid
						551.1234	$[2M+Na-caffeic]^+$				191.0561	$[Quin-H]^-$ *(100)*	
						377.0846	$[M+Na]^+$						
						163.0421	$[Caffeoyl+H]^+$						
						145.0279	$[Caffeoyl+H-H_2O]^+$						
						135.0433	$[Caffeoyl+H-CO]^+$						
						117.0342	$[Caffeoyl+H-CO-H_2O]^+$						
						89.0396	$[Caffeoyl+H-H_2O-2CO]^+$						
3	7.32	300 sh, 324	355.1026	–0.3	$C_{16}H_{19}O_9$	731.1791	$[2M+Na]^+$	353.0869	–0.4	$C_{16}H_{17}O_9$	707.1821	$[2M-H]^-$	5–*trans*–*O*–Caffeoylquinic acid
						551.1234	$[2M+Na-caffeic]^+$				191.0556	$[Quin-H]^-$ *(100)*	
						377.0846	$[M+Na]^+$				179.0343	$[Caffeic-H]^-$ *(1)*	
						163.0421	$[Caffeoyl+H]^+$				173.0449	$[Quin-H-H_2O]^-$ *(3)*	
						145.0279	$[Caffeoyl+H-H_2O]^+$				135.0443	$[Caffeic-H-CO_2]^-$ *(2)*	
						135.0433	$[Caffeoyl+H-CO]^+$						
						117.0342	$[Caffeoyl+H-CO-H_2O]^+$						
						89.0396	$[Caffeoyl+H-H_2O-2CO]^+$						
4	8.12	–	355.1068	3.9	$C_{16}H_{19}O_9$	731.1739	$[2M+Na]^+$	353.0861	–1.2	$C_{16}H_{17}O_9$	707.1796	$[2M-H]^-$	3–*cis*–*O*–Caffeoylquinic acid
						709.1981	$[2M+H]^+$				191.0557	$[Quin-H]^-$ *(100)*	
						163.0397	$[Caffeoyl+H]^+$				179.0344	$[Caffeic-H]^-$ *(12)*	
						145.0128	$[Caffeoyl+H-H_2O]^+$				135.0441	$[Caffeic-H-CO_2]^-$ *(21)*	
						135.0463	$[Caffeoyl+H-CO]^+$						
						117.0333	$[Caffeoyl+H-CO-H_2O]^+$						
						89.0383	$[Caffeoyl+H-H_2O-2CO]^+$						
5	8.36	–	355.1068	3.9	$C_{16}H_{19}O_9$	377.0844	$[M+Na]^+$	353.0865	–0.8	$C_{16}H_{17}O_9$	191.0554	$[Quin-H]^-$ *(100)*	4–*trans*–*O*–Caffeoylquinic acid
						163.0445	$[Caffeoyl+H]^+$				173.0458	$[Quin-H-H_2O]^-$ *(13)*	
						145.0325	$[Caffeoyl+H-H_2O]^+$						
						135.0408	$[Caffeoyl+H-CO]^+$						
						117.0364	$[Caffeoyl+H-CO-H_2O]^+$						
6	10.23	301 sh, 316	355.1068	3.9	$C_{16}H_{19}O_9$	731.1746	$[2M+Na]^+$	353.0867	–0.6	$C_{16}H_{17}O_9$	707.1816	$[2M-H]^-$	5–*cis*–*O*–Caffeoylquinic acid
						551.1199	$[2M+Na-caffeic]^+$				191.0557	$[Quin-H]^-$ *(100)*	
						377.0841	$[M+Na]^+$				173.0449	$[Quin-H-H_2O]^-$ *(3)*	
						163.0400	$[Caffeoyl+H]^+$						
						145.0284	$[Caffeoyl+H-H_2O]^+$						
						135.0443	$[Caffeoyl+H-CO]^+$						
						117.0346	$[Caffeoyl+H-CO-H_2O]^+$						
						89.0396	$[Caffeoyl+H-H_2O-2CO]^+$						
7	15.06	–			$C_{16}H_{19}O_9$	163.0399	$[Caffeoyl+H]^+$	353.0876	0.3	$C_{16}H_{17}O_9$	191.0578	$[Quin-H]^-$ *(100)*	4–*cis*–*O*–Caffeoylquinic acid
						145.0287	$[Caffeoyl+H-H_2O]^+$				179.0314	$[Caffeic-H]^-$ *(5)*	
						135.0446	$[Caffeoyl+H-CO]^+$				173.0455	$[Quin-H-H_2O]^-$ *(2)*	
						117.0278	$[Caffeoyl+H-CO-H_2O]^+$						

	LC	DAD	ESI(+)–QToF/MS					ESI(–)–QToF/MS					Assignment
Nº	Rt (min)	UV bands (nm)	Exp. Acc. Mass $[M+H]^+$	Error (mDa)	Formula $[M+H]^+$	Adducts & fragment ions of $[M+H]^+$ *m/z*		Exp. Acc. Mass $[M-H]^-$	Error (mDa)	Formula $[M-H]^-$	Adducts & fragment ions of $[M-H]^-$ *m/z*		Tentative identification
p-Coumaroylquinic acids													
8	9.82	312	339.1075	–0.5	$C_{16}H_{19}O_8$	699.1888	$[2M+Na]^+$	337.0921	–0.2	$C_{16}H_{17}O_8$	675.1904	$[2M-H]^-$	3–*p*–Coumaroylquinic acid
						361.0892	$[M+Na]^+$				191.0467	$[Quin-H]^-$	
						147.0451	$[p\text{Coumaroyl+H}]^+$				163.0393	$[p\text{Coumaric-H}]^-$	
						119.0500	$[p\text{Coumaroyl+H-CO}]^+$				119.0496	$[p\text{Coumaric-H-CO}_2]^-$	
						91.0556	$[p\text{Coumaroyl+H-2CO}]^+$						
9	13.74	308	339.1133	5.3	$C_{16}H_{19}O_8$	699.1916	$[2M+Na]^+$	337.0919	–0.4	$C_{16}H_{17}O_8$	191.0553	$[Quin-H]^-$	5–*p*–Coumaroylquinic acid
						361.0907	$[M+Na]^+$				173.0449	$[Quin-H-H_2O]^-$	
						147.0453	$[p\text{Coumaroyl+H-H}_2\text{O}]^+$				163.0390	$[p\text{Coumaric-H}]^-$	
						119.0500	$[p\text{Coumaroyl+H-H}_2\text{O-CO}]^+$				119.0491	$[p\text{Coumaric-H-CO}_2]^-$	
						91.0561	$[p\text{Coumaroyl+H-H}_2\text{O-2CO}]^+$						
Caffeoyltartaric acid													
10	9.06	301 sh, 323			$C_{13}H_{13}O_9$			311.0526	–12.3	$C_{13}H_{11}O_9$	293.0287	$[Caftar-H-H_2O]^-$	Caffeoyltartaric acid
											179.0349	$[Caffeic-H]^-$	
											149.0227	$[Tartaric-H]^-$	
											135.0432	$[Caffeic-H-CO_2]^-$	
p-Coumaroyltartaric acid													
11	15.63	310			$C_{13}H_{13}O_8$			295.0457	–0.3	$C_{13}H_{11}O_8$	163.0393	$[p\text{Coumaric-H}]^-$	*p*–Coumaroyltartaric acid
											149.0104	$[Tartaric-H]^-$	
											119.0481	$[p\text{Coumaric-H-CO}_2]^-$	
Caffeoylmalic acid													
12	9.05	301 sh, 323	297.0585	–2.5	$C_{13}H_{13}O_8$	319.0429	$[M+Na]^+$	295.0448	–0.6	$C_{13}H_{11}O_8$	591.0983	$[2M-H]^-$	Caffeoylmalic acid
						163.0404	$[Caffeoyl+H]^+$				179.0345	$[Caffeic-H]^-$	
						145.0297	$[Caffeoyl+H-H_2O]^+$				135.0446	$[Caffeic-H-CO_2]^-$	
						135.0447	$[Caffeoyl+H-CO]^+$				133.0275	$[Malic-H]^-$	
						117.0348	$[Caffeoyl+H-CO-H_2O]^+$				115.0032	$[Malic-H-H_2O]^-$	
						89.0397	$[Caffeoyl+H-H_2O-2CO]^+$				105.0342	$[Malic-H-CO]^-$	
Dicaffeoylquinic acids and caffeoylquinic acid glycosides													
13	5.86	–	517.1548	0.9	$C_{22}H_{29}O_{14}$	539.1364	$[M+Na]^+$	515.1402	0.1	$C_{22}H_{27}O_{14}$	353.0869	$[Cafquin-H]^-$	Caffeoylquinic acid–hexoside
						355.1038	$[M-hexosyl]^+$				191.0548	$[Quin-H]^-$	
						163.0415	$[Caffeoyl+H]^+$						
						145.0310	$[Caffeoyl+H-H_2O]^+$						
						135.0449	$[Caffeoyl+H-CO]^+$						
						117.0385	$[Caffeoyl+H-CO-H_2O]^+$						
						89.0399	$[Caffeoyl+H-H_2O-2CO]^+$						
14	7.56	–			$C_{22}H_{29}O_{14}$	539.1367	$[M+Na]^+$	515.1402	0.1	$C_{22}H_{27}O_{14}$			Caffeoylquinic acid–hexoside
15	20.20	321	517.1423	7.7	$C_{25}H_{25}O_{12}$	539.1155	$[M+Na]^+$	515.1194	0.4	$C_{25}H_{23}O_{12}$	353.0871	$[Cafquin-H]^-$	1,5–di–*O*–Caffeoylquinic acid
						499.1237	$[M+H-H_2O]^+$				335.0771	$[Cafquin-H-H_2O]^-$	
						355.0985	$[Cafquin+H]^+$				191.0558	$[Quin-H]^-$	
						163.0403	$[Caffeoyl+H]^+$				179.0349	$[Caffeic-H]^-$	
						145.0159	$[Caffeoyl+H-H_2O]^+$				135.0448	$[Caffeic-H-CO_2]^-$	
						135.0451	$[Caffeoyl+H-CO]^+$						
						117.0350	$[Caffeoyl+H-CO-H_2O]^+$						
						89.0404	$[Caffeoyl+H-H_2O-2CO]^+$						
16	20.63	326	517.1332	–1.4	$C_{25}H_{25}O_{12}$	539.1155	$[M+Na]^+$	515.1186	–0.4	$C_{25}H_{23}O_{12}$	353.0866	$[Cafquin-H]^-$	3,5–di–*O*–Caffeoylquinic acid
						499.1230	$[M+H-H_2O]^+$				335.0761	$[Cafquin-H-H_2O]^-$	
						355.1016	$[Cafquin+H]^+$				191.0556	$[Quin-H]^-$	
						163.0401	$[Caffeoyl+H]^+$				179.0347	$[Caffeic-H]^-$	
						145.0291	$[Caffeoyl+H-H_2O]^+$				135.0446	$[Caffeic-H-CO_2]^-$	
						135.0450	$[Caffeoyl+H-CO]^+$						
						117.0346	$[Caffeoyl+H-CO-H_2O]^+$						
						89.0401	$[Caffeoyl+H-H_2O-2CO]^+$						

	LC	DAD	ESI(+)–QToF/MS					ESI(–)–QToF/MS					Assignment
Nº	Rt (min)	UV bands (nm)	Exp. Acc. Mass $[M+H]^+$	Error (mDa)	Formula $[M+H]^+$	Adducts & fragment ions of $[M+H]^+$ *m/z*		Exp. Acc. Mass $[M-H]^-$	Error (mDa)	Formula $[M-H]^-$	Adducts & fragment ions of $[M-H]^-$ *m/z*		Tentative identification
17	24.17	331	517.1423	7.7	$C_{25}H_{25}O_{12}$	539.1165	$[M+Na]^+$	515.1190	0.0	$C_{25}H_{23}O_{12}$	353.0860	[Cafquin–H]$^-$	4,5–di–*O*–Caffeoylquinic acid
						499.1228	$[M+H-H_2O]^+$				335.0802	[Cafquin–H–H_2O]$^-$	
						473.2006	$[M+H-CO_2]^+$				179.0347	[Caffeic–H]$^-$	
						355.0161	[Cafquin+H]$^+$				173.0449	[Quin–H–H_2O]$^-$	
						163.0395	[Caffeoyl+H]$^+$				135.0441	[Caffeic–H–CO_2]$^-$	
						135.0447	[Caffeoyl+H–CO]$^+$						
						117.0347	[Caffeoyl+H–CO–H_2O]$^+$						
						89.0400	[Caffeoyl+H–H_2O–2CO]$^+$						
p-Coumaroylcaffeoylquinic acids													
18	23.58	312	501.1384	1.3	$C_{25}H_{25}O_{11}$	523.1219	$[M+Na]^+$	499.1233	0.7	$C_{25}H_{23}O_{11}$	353.0868	[M–H–coumaroyl]$^-$	3–*p*–Coumaroyl–4–caffeoylquinic acid
						483.1295	$[M+H-H_2O]^+$				337.0916	[M–H–caffeoyl]$^-$	
						163.0399	[Caffeoyl+H–H_2O]$^+$				191.0560	[Quin–H]$^-$	
						147.0446	[*p*Coumaroyl+H]$^+$				179.0353	[Caffeic–H]$^-$	
						145.0279	[Caffeoyl+H–2H_2O]$^+$				163.0398	[*p*Coumaric–H]$^-$	
						135.0455	[Caffeoyl+H–H_2O–CO]$^+$				135.0452	[Caffeic–H–CO_2]$^-$	
						119.0497	[*p*Coumaroyl+H–H_2O–CO]$^+$				119.0503	[*p*Coumaric–H–CO_2]$^-$	
						117.0335	[Caffeoyl+H–2H_2O–CO]$^+$						
						91.0550	[*p*Coumaroyl+H–H_2O–2CO]$^+$						
						89.0398	[Caffeoyl+H–2H_2O–2CO]$^+$						
19	23.95	316	501.1377	2.0	$C_{25}H_{25}O_{11}$	523.1216	$[M+Na]^+$	499.1241	–0.1	$C_{25}H_{23}O_{11}$	353.0852	[M–H–coumaroyl]$^-$	4–Caffeoyl–5–*p*–coumaroylquinic acid
						483.1281	$[M+H-H_2O]^+$				337.0928	[M–H–caffeoyl]$^-$	
						147.0445	[*p*Coumaroyl+H]$^+$				191.0553	[Quin–H]$^-$	
						119.0493	[*p*Coumaroyl+H–CO]$^+$				179.0342	[Caffeic–H]$^-$	
						91.0550	[*p*Coumaroyl+H–2CO]$^+$				163.0390	[*p*Coumaric–H]$^-$	
											135.0448	[Caffeic–H–CO_2]$^-$	
											119.0490	[*p*Coumaric–H–CO_2]$^-$	
Dicaffeoyltartaric acids													
20	10.53	301 sh, 324			$C_{22}H_{19}O_{12}$	497.0677	$[M+Na]^+$	473.0719	–0.1	$C_{22}H_{17}O_{12}$	947.1354	[2M–H]$^-$	di–*O*–Caffeoyltartaric acid
						457.0698	$[M+H-H_2O]^+$				311.0402	[Caftar–H]$^-$	
						295.0577	[Caftar–H–H_2O]$^+$				293.0296	[Caftar–H–H_2O]$^-$	
						163.0397	[Caffeoyl+H]$^+$				179.0345	[Caffeic–H]$^-$	
						145.0292	[Caffeoyl+H–H_2O]$^+$				149.0091	[Tartaric–H]$^-$	
						135.0448	[Caffeoyl+H–CO]$^+$				135.0443	[Caffeic–H–CO_2]$^-$	
						117.0343	[Caffeoyl+H–CO–H_2O]$^+$				105.0339	[Tartaric–H–CO_2]$^-$	
						89.0396	[Caffeoyl+H–H_2O–2CO]$^+$						
21	12.54	301 sh, 323			$C_{22}H_{19}O_{12}$	295.0563	[Caftar–H–H_2O]$^+$	473.0713	–0.7	$C_{22}H_{17}O_{12}$	311.0387	[Caftar–H]$^-$	*meso*–di–*O*–Caffeoyltartaric acid
						163.0398	[Caffeoyl+H]$^+$				293.0297	[Caftar–H–H_2O]$^-$	
						145.0288	[Caffeoyl+H–H_2O]$^+$				179.0346	[Caffeic–H]$^-$	
						135.0446	[Caffeoyl+H–CO]$^+$				149.0126	[Tartaric–H]$^-$	
						117.0341	[Caffeoyl+H–CO–H_2O]$^+$				135.0448	[Caffeic–H–CO_2]$^-$	
						89.0398	[Caffeoyl+H–H_2O–2CO]$^+$				105.0343	[Tartaric–H–CO_2]$^-$	
Other hydroxycinnamic acid derivatives													
22	5.39	–	343.1098	6.9	$C_{15}H_{19}O_9$	365.0878	$[M+Na]^+$	341.0905	–3.2	$C_{15}H_{17}O_9$			Caffeic acid–hexoside
						163.0394	[Caffeoyl+H]$^+$						
						145.0104	[Caffeoyl+H–H_2O]$^+$						
						135.0497	[Caffeoyl+H–CO]$^+$						
						89.0401	[Caffeoyl+H–H_2O–2CO]$^+$						
23	5.64	–			$C_{15}H_{19}O_9$	365.0833	$[M+Na]^+$	341.0854	1.9	$C_{15}H_{17}O_9$	179.0330	[Caffeic–H]$^-$	Caffeic acid–hexoside
						163.0389	[Caffeoyl+H]$^+$				135.0435	[Caffeic–H–CO_2]$^-$	
						145.0289	[Caffeoyl+H–H_2O]$^+$						
						135.0473	[Caffeoyl+H–CO]$^+$						
						117.0309	[Caffeoyl+H–CO–H_2O]$^+$						
24	6.08	301 sh, 325			$C_{15}H_{19}O_9$	365.0844	$[M+Na]^+$	341.0873	0.0	$C_{15}H_{17}O_9$	179.0348	[Caffeic–H]$^-$	Caffeic acid–hexoside
											135.0452	[Caffeic–H–CO_2]$^-$	

	LC	DAD	ESI(+)–QToF/MS					ESI(–)–QToF/MS					Assignment
Nº	Rt (min)	UV bands (nm)	Exp. Acc. Mass $[M+H]^+$	Error (mDa)	Formula $[M+H]^+$	Adducts & fragment ions of $[M+H]^+$ *m/z*		Exp. Acc. Mass $[M-H]^-$	Error (mDa)	Formula $[M-H]^-$	Adducts & fragment ions of $[M-H]^-$ *m/z*		Tentative identification
25	7.69	–			$C_{15}H_{19}O_9$	365.0843	$[M+Na]^+$	341.0876	–0.3	$C_{15}H_{17}O_9$	179.0351	$[Caffeic–H]^-$	Caffeic acid–hexoside
											135.0449	$[Caffeic–H–CO_2]^-$	
26	8.44	–			$C_{15}H_{19}O_9$	365.0855	$[M+Na]^+$	341.0867	0.6	$C_{15}H_{17}O_9$	179.0349	$[Caffeic–H]^-$	Caffeic acid–hexoside
						163.0405	$[Caffeoyl+H]^+$				135.0432	$[Caffeic–H–CO_2]^-$	
						145.0137	$[Caffeoyl+H–H_2O]^+$						
						135.0455	$[Caffeoyl+H–CO]^+$						
						117.0343	$[Caffeoyl+H–CO–H_2O]^+$						
						89.0383	$[Caffeoyl+H–H_2O–2CO]^+$						
27	9.01	–			$C_{15}H_{19}O_9$			341.0897	–2.4	$C_{15}H_{17}O_9$	179.0349	$[Caffeic–H]^-$	Caffeic acid–hexoside
											135.0432	$[Caffeic–H–CO_2]^-$	
28	9.52	–			$C_{15}H_{19}O_9$	365.0837	$[M+Na]^+$	341.0883	–1.0	$C_{15}H_{17}O_9$	179.0355	$[Caffeic–H]^-$	Caffeic acid–hexoside
						145.0078	$[Caffeoyl+H–H_2O]^+$				135.0448	$[Caffeic–H–CO_2]^-$	
						135.0471	$[Caffeoyl+H–CO]^+$						
						117.0334	$[Caffeoyl+H–CO–H_2O]^+$						
						89.0275	$[Caffeoyl+H–H_2O–2CO]^+$						
29	9.64	–			$C_{15}H_{19}O_9$	163.0380	$[Caffeoyl+H]^+$	341.0897	–2.4	$C_{15}H_{17}O_9$	135.0442	$[Caffeic–H–CO_2]^-$	Caffeic acid–hexoside
						145.0338	$[Caffeoyl+H–H_2O]^+$						
						135.0482	$[Caffeoyl+H–CO]^+$						
						117.0348	$[Caffeoyl+H–CO–H_2O]^+$						
						89.0275	$[Caffeoyl+H–H_2O–2CO]^+$						
30	8.01	301 sh, 325	359.0802	3.5	$C_{18}H_{15}O_8$	163.0415	$[Caffeoyl+H]^+$	357.0633	–2.3	$C_{18}H_{13}O_8$			Caffeoyl–derivative
						145.0640	$[Caffeoyl+H–H_2O]^+$						
						135.0390	$[Caffeoyl+H–CO]^+$						
						117.0346	$[Caffeoyl+H–CO–H_2O]^+$						
						89.0407	$[Caffeoyl+H–H_2O–2CO]^+$						
31	6.03	301 sh, 326			$C_{17}H_{23}O_{10}$	409.1092	$[M+Na]^+$	385.1138	–0.3	$C_{17}H_{21}O_{10}$	208.0659	$[M–H–hexosyl–CH_3]^-$	Sinapic acid–hexoside
						225.0745	$[M+H–hexosyl]^+$				179.0350	$[M–H–hexosyl–CO_2]^-$	
											164.0519	$[M–H–hexosyl–CH_3–CO_2]^-$	
											149.0620	$[M–H–hexosyl–2CH_3–CO_2]^-$	
32	9.70	–			$C_{17}H_{23}O_{10}$	409.0938	$[M+Na]^+$	385.1117	1.8	$C_{17}H_{21}O_{10}$	223.0605	$[M–H–hexosyl]^-$	Sinapic acid–hexoside
						225.0774	$[M+H–hexosyl]^+$				208.0372	$[M–H–hexosyl–CH_3]^-$	
						207.0665	$[M+H–hexosyl–H_2O]^+$				179.0725	$[M–H–hexosyl–CO_2]^-$	
						192.0411	$[M+H–hexosyl–H–CH_3OH]^+$				164.0486	$[M–H–hexosyl–CH_3–CO_2]^-$	
						175.0411	$[M+H–hexosyl–H_2O–CH_3OH]^+$				149.0222	$[M–H–hexosyl–2CH_3–CO_2]^-$	
						129.0381	$[M+H–hexosyl–2H_2O–CO–CH_3OH]^+$						
33	10.36	–			$C_{17}H_{23}O_{10}$	409.1115	$[M+Na]^+$	385.1124	1.1	$C_{17}H_{21}O_{10}$			Sinapic acid–hexoside
						192.0430	$[M+H–hexosyl–H–CH_3OH]^+$						
34	13.13	–			$C_{17}H_{23}O_{10}$	409.1111	$[M+Na]^+$	385.1112	2.3	$C_{17}H_{21}O_{10}$	223.0598	$[M–H–hexosyl]^-$	Sinapic acid–hexoside
						225.0753	$[M+H–hexosyl]^+$				208.0365	$[M–H–hexosyl–CH_3]^-$	
						207.0620	$[M+H–hexosyl–H_2O]^+$				179.0576	$[M–H–hexosyl–CO_2]^-$	
						192.0416	$[M+H–hexosyl–H–CH_3OH]^+$				164.0473	$[M–H–hexosyl–CH_3–CO_2]^-$	
						175.0461	$[M+H–hexosyl–H_2O–CH_3OH]^+$				149.0234	$[M–H–hexosyl–2CH_3–CO_2]^-$	
						129.0322	$[M+H–hexosyl–2H_2O–CO–CH_3OH]^+$						
35	8.32	–			$C_{15}H_{19}O_8$	349.0901	$[M+Na]^+$	325.0914	0.9	$C_{15}H_{17}O_8$	163.0397	$[M–H–hexosyl]^-$	*p*–Coumaric acid–hexoside
						147.0449	$[p\text{Coumaroyl}+H–H_2O]^+$				119.0493	$[M–H–hexosyl–CO_2]^-$	
						119.0506	$[p\text{Coumaroyl}+H–H_2O–CO]^+$						
						91.0569	$[p\text{Coumaroyl}+H–H_2O–2CO]^+$						
36	3.70	–			$C_{15}H_{21}O_9$			343.1029	0.0	$C_{15}H_{19}O_9$	181.0496	$[DihydroCaf–H]^-$	Dihydrocaffeic acid–hexoside
						367.0989	$[M+Na]^+$				163.0393	$[DihydroCaf–H–H_2O]^-$	
											135.0450	$[DihydroCaf–H–H_2O–CO]^-$	
											119.0489	$[DihydroCaf–H–H_2O–CO_2]^-$	
37	3.83	–			$C_{15}H_{21}O_9$			343.1028	0.1	$C_{15}H_{19}O_9$	181.0504	$[DihydroCaf–H]^-$	Dihydrocaffeic acid–hexoside
						367.0999	$[M+Na]^+$				163.0398	$[DihydroCaf–H–H_2O]^-$	
											135.0450	$[DihydroCaf–H–H_2O–CO]^-$	
											119.0492	$[DihydroCaf–H–H_2O–CO_2]^-$	

	LC	DAD	ESI(+)–QToF/MS					ESI(–)–QToF/MS					Assignment
Nº	Rt (min)	UV bands (nm)	Exp. Acc. Mass $[M+H]^+$	Error (mDa)	Formula $[M+H]^+$	Adducts & fragment ions of $[M+H]^+$ *m/z*		Exp. Acc. Mass $[M-H]^-$	Error (mDa)	Formula $[M-H]^-$	Adducts & fragment ions of $[M-H]^-$ *m/z*		Tentative identification
38	11.81	307			$C_{11}H_{13}O_4$			207.0650	0.7	$C_{11}H_{11}O_4$	192.0422	$[M-H-CH_3]^-$	Ferulic acid methyl ester
39	14.47	–			$C_{11}H_{13}O_4$			207.0663	–0.6	$C_{11}H_{11}O_4$	192.0422	$[M-H-CH_3]^-$	Ferulic acid methyl ester
											177.0206	$[M-H-2CH_3]^-$	
											133.0685	$[M-H-CH_3-CO_2]^-$	
40	16.48	–			$C_{11}H_{13}O_4$			207.0656	0.1	$C_{11}H_{11}O_4$	192.0435	$[M-H-CH_3]^-$	Ferulic acid methyl ester
											177.0206	$[M-H-2CH_3]^-$	
											133.0686	$[M-H-CH_3-CO_2]^-$	
Hydroxybenzoic acid derivatives													
41	4.67	–		3.6	$C_7H_6O_4$	138.0281	$[M]^+$	137.0238	0.1	$C_7H_5O_3$	109.0294	$[M-H-CO]^-$	Hydroxybenzoic acid
											93.0331	$[M-H-CO_2]^-$	
42	5.42	–			$C_7H_7O_4$			153.0196	–0.8	$C_7H_5O_4$	135.0448	$[DiHBZ-H-H_2O]^-$	Dihydroxybenzoic acid
											109.0294	$[M-H-CO_2]^-$	
43	4.22	–			$C_{13}H_{17}O_8$			299.0733	3.4	$C_{13}H_{15}O_8$	271.0141	$[M-H-CO]^-$	Hydroxybenzoic acid–hexoside
											137.0216	$[HBZ-H]^-$	
											93.0498	$[HBZ-H-CO_2]^-$	
44	5.15	–			$C_{13}H_{17}O_8$			299.0764	0.3	$C_{13}H_{15}O_8$	137.0244	$[HBZ-H]^-$	Hydroxybenzoic acid–hexoside
45	2.49	–			$C_{13}H_{17}O_9$			315.0714	0.2	$C_{13}H_{15}O_9$	153.0181	$[DiHBZ-H]^-$	Dihydroxybenzoic acid–hexoside
											152.0114	$[DiHBZ-2H]^-$	
											135.0441	$[DiHBZ-H-H_2O]^-$	
											109.0283	$[DiHBZ-H-CO_2]^-$	
46	2.69	–			$C_{13}H_{17}O_9$			315.0714	0.2	$C_{13}H_{15}O_9$	153.0181	$[DiHBZ-H]^-$	Dihydroxybenzoic acid–hexoside
											152.0114	$[DiHBZ-2H]^-$	
											135.0441	$[DiHBZ-H-H_2O]^-$	
											109.0283	$[DiHBZ-H-CO_2]^-$	
47	3.74	–			$C_{13}H_{17}O_9$			315.0716	0.0	$C_{13}H_{15}O_9$	153.0185	$[DiHBZ-H]^-$	Dihydroxybenzoic acid–hexoside
											109.0287	$[DiHBZ-H-CO_2]^-$	
48	3.91	–			$C_{13}H_{17}O_9$			315.0716	0.0	$C_{13}H_{15}O_9$	153.0172	$[DiHBZ-H]^-$	Dihydroxybenzoic acid–hexoside
											109.0307	$[DiHBZ-H-CO_2]^-$	
49	4.48	–			$C_{13}H_{17}O_9$			315.0716	0.0	$C_{13}H_{15}O_9$	153.0172	$[DiHBZ-H]^-$	Dihydroxybenzoic acid–hexoside
											152.0108	$[DiHBZ-2H]^-$	
											135.0441	$[DiHBZ-H-H_2O]^-$	
											109.0261	$[DiHBZ-H-CO_2]^-$	
50	4.68	–			$C_{13}H_{17}O_9$			315.0717	–0.1	$C_{13}H_{15}O_9$	153.0196	$[DiHBZ-H]^-$	Dihydroxybenzoic acid–hexoside
											135.0442	$[DiHBZ-H-H_2O]^-$	
											109.0298	$[DiHBZ-H-CO_2]^-$	
51	2.80	–						331.0661	–0.4	$C_{13}H_{15}O_{10}$	313.0557	$[M-H-H_2O]^-$	Gallic acid–hexoside
											169.0113	$[Gallic-H]^-$	
											168.0057	$[Gallic-2H]^-$	
											149.9953	$[Gallic-2H-H_2O]^-$	
											125.0226	$[Gallic-H-CO_2]^-$	
52	2.88	–						331.0661	–0.4	$C_{13}H_{15}O_{10}$	313.0557	$[M-H-H_2O]^-$	Gallic acid–hexoside
											169.0113	$[Gallic-H]^-$	
											168.0057	$[Gallic-2H]^-$	
											149.9953	$[Gallic-2H-H_2O]^-$	
											125.0226	$[Gallic-H-CO_2]^-$	
53	6.61	–						331.0660	0.5	$C_{13}H_{15}O_{10}$	313.0544	$[M-H-H_2O]^-$	Gallic acid–hexoside
											169.0140	$[Gallic-H]^-$	
											168.0054	$[Gallic-2H]^-$	
											149.9953	$[Gallic-2H-H_2O]^-$	
											125.0232	$[Gallic-H-CO_2]^-$	
54	5.90	–	361.1107	2.8	$C_{15}H_{21}O_{10}$	97.0288	$[M+H-glucosyl-2CH_3-CO-CO_2]^+$	359.0975	0.3	$C_{15}H_{19}O_{10}$	197.0454	$[M-H-glucosyl]^-$	Syringic acid–hexoside
											182.0210	$[M-H-glucosyl-CH_3]^-$	
											153.0561	$[M-H-glucosyl-CO_2]^-$	
											138.0337	$[M-H-glucosyl-CH_3-CO_2]^-$	
											123.0105	$[M-H-glucosyl-2CH_3-CO_2]^-$	

Nº	LC Rt (min)	DAD UV bands (nm)	ESI(+)–QToF/MS Exp. Acc. Mass $[M+H]^+$	Error (mDa)	Formula $[M+H]^+$	Adducts & fragment ions of $[M+H]^+$ *m/z*		ESI(–)–QToF/MS Exp. Acc. Mass $[M–H]^–$	Error (mDa)	Formula $[M–H]^–$	Adducts & fragment ions of $[M–H]^–$ *m/z*		Assignment Tentative identification
55	17.09	–			$C_{20}H_{21}O_{12}$			451.0880	–0.3	$C_{20}H_{19}O_{12}$	331.0682	$[M–H]^–$	Hydroxybenzoyl gallic acid–hexoside
											313.0558	$[M–H–H_2O]^–$	
											168.0060	$[Gallic–2H]^–$	
											124.0160	$[Gallic–2H–CO_2]^–$	
56	24.83	–			$C_{20}H_{21}O_{12}$			451.0865	1.2	$C_{20}H_{19}O_{12}$	331.0660	$[M–H]^–$	Hydroxybenzoyl gallic acid–hexoside
											313.0544	$[M–H–H_2O]^–$	
											168.0054	$[Gallic–2H]^–$	
											124.0163	$[Gallic–2H–CO_2]^–$	
57	17.68	–			$C_{20}H_{21}O_{11}$			435.0933	–0.6	$C_{20}H_{19}O_{11}$	315.0722	$[DiHBZhex–H]^–$ or $[M–OC_6H_4CO]^–$	Hydroxybenzoyl–*O*–dihydroxybenzoic acid-hexoside
											153.0184	$[DiHBZ–H]^–$	
											152.0126	$[DiHBZ–2H]^–$	
											137.0258	$[HBZ–H]^–$	
											108.0227	$[DiHBZ–2H–CO_2]^–$	
											93.0344	$[HBZ–H–CO_2]^–$	
58	19.41	–			$C_{20}H_{21}O_{11}$			435.0927	0.0	$C_{20}H_{19}O_{11}$	315.0710	$[DiHBZhex–H]^–$ or $[M–OC_6H_4CO]^–$	Hydroxybenzoyl–*O*–dihydroxybenzoic acid-hexoside
											153.0192	$[DiHBZ–H]^–$	
											108.0189	$[DiHBZ–2H–CO_2]^–$	
59	23.64	–			$C_{20}H_{21}O_{11}$			435.0920	0.7	$C_{20}H_{19}O_{11}$			Hydroxybenzoyl–*O*–dihydroxybenzoic acid-hexoside
60	26.88	256,			$C_{20}H_{21}O_{11}$			435.0925	0.2	$C_{20}H_{19}O_{11}$	315.0471	$[DiHBZhex–H]^–$ or $[M–OC_6H_4CO]^–$	Hydroxybenzoyl–*O*–dihydroxybenzoic acid-hexoside
		335 sh									297.0611	$[DiHBZhex–H–H_2O]^–$	
											152.0117	$[DiHBZ–2H]^–$	
											137.0238	$[HBZ–H]^–$	
											108.0215	$[DiHBZ–2H–CO_2]^–$	
											93.0337	$[HBZ–H–CO_2]^–$	
61	27.09	–			$C_{20}H_{21}O_{11}$			435.0927	0.0	$C_{20}H_{19}O_{11}$	315.0715	$[DiHBZhex–H]^–$ or $[M–OC_6H_4CO]^–$	Hydroxybenzoyl–*O*–dihydroxybenzoic acid-hexoside
											297.0609	$[DiHBZhex–H–H_2O]^–$	
											153.0195	$[DiHBZ–H]^–$	
											137.0240	$[HBZ–H]^–$	
											108.0215	$[DiHBZ–2H–CO_2]^–$	
											93.0341	$[HBZ–H–CO_2]^–$	
Hydroxyphenylacetic derivatives													
62	5.60	–			$C_8H_9O_3$			151.0392	0.3	$C_8H_7O_3$	123.0439	$[M–H–CO]^–$	4–hydroxyphenylacetic acid
											107.0500	$[M–H–CO_2]^–$	
63	5.20	270,			$C_{14}H_{19}O_8$			313.0923	0.0	$C_{14}H_{17}O_8$	151.0399	$[M–H–glucosyl]^–$	4–hydroxyphenylacetic acid–hexoside
		276 sh									123.0447	$[M–H–glucosyl–CO]^–$	
											107.0499	$[M–H–glucosyl–CO_2]^–$	
Flavonoids													
Flavonols													
64	17.16	279,	465.1022	–1.1	$C_{21}H_{21}O_{12}$	487.0832	$[M+Na]^+$	463.0874	–0.3	$C_{21}H_{19}O_{12}$	301.0341	$[Y_0]^–$	Quercetin–*O*–hexoside
		344				303.0501	$[Y_0]^+$				255.0237	$[Y_0–CHO–OH]^–$	
						145.0090	$[Y_0–CHO–OH–4CO]^+$				227.0332	$[Y_0–2CO–H_2O]^–$	
											151.0027	$[^{1,3}A]^–$	
											133.0685		
65	18.03	252,	465.1007	–2.6	$C_{21}H_{21}O_{12}$	487.0834	$[M+Na]^+$	463.0888	1.1	$C_{21}H_{19}O_{12}$	301.0356	$[Y_0]^–$	Quercetin–*O*–hexoside
		367				303.0465	$[Y_0]^+$				255.0310	$[Y_0–CHO–OH]^–$	
						229.0492	$[Y_0–CHO–OH–CO]^+$				151.0037	$[^{1,3}A]^–$	
						153.0186	$[^{1,3}A]^+$				107.0137	$[^{0,2}A–2CO]^–$;$[^{0,2}B–CO]^–$	
66	20.25	252,	465.1032	–0.1	$C_{21}H_{21}O_{12}$	487.0840	$[M+Na]^+$	463.0880	0.3	$C_{21}H_{19}O_{12}$	301.0339	$[Y_0]^–$	Quercetin 3–*O*–galactoside
		330				303.0504	$[Y_0]^+$				255.0303	$[Y_0–CHO–OH]^–$	
						229.0492	$[Y_0–CHO–OH–CO]^+$				151.0039	$[^{1,3}A]^–$	

	LC	DAD	ESI(+)–QToF/MS					ESI(–)–QToF/MS					Assignment
Nº	Rt (min)	UV bands (nm)	Exp. Acc. Mass $[M+H]^+$	Error (mDa)	Formula $[M+H]^+$	Adducts & fragment ions of $[M+H]^+$ *m/z*		Exp. Acc. Mass $[M–H]^–$	Error (mDa)	Formula $[M–H]^–$	Adducts & fragment ions of $[M–H]^–$ *m/z*		Tentative identification
67	18.44	254, 349	479.0826	0.0	$C_{21}H_{19}O_{13}$	501.0644	$[M+Na]^+$	477.0675	1.1	$C_{21}H_{17}O_{13}$	301.0347	$[Y_0]^–$	Quercetin–3–*O*–glucuronide
						303.0507	$[Y_0]^+$				255.0293	$[Y_0–CHO–OH]^–$	
						257.0443	$[Y_0–CHO–OH]^+$				227.0346	$[Y_0–2CO–H_2O]^–$	
						153.0186	$[^{1,3}A]^+$				151.0036	$[^{1,3}A]^–$	
68	9.50	256, 352	641.1385	3.1	$C_{27}H_{29}O_{18}$	663.1232	$[M+Na]^+$	639.1168	–2.9	$C_{27}H_{27}O_{18}$	463.0865	$[Y_1]^–$	Quercetin hexose–glucuronide
						303.0515	$[Y_0]^+$				301.0360	$[Y_0]^–$	
											135.0432	$[^{0,2}A–CO]^–;[^{0,2}B]^–$	
69	10.58	–	641.1385	3.1	$C_{27}H_{29}O_{18}$	663.1232	$[M+Na]^+$	639.1168	–2.9	$C_{27}H_{27}O_{18}$	463.0865	$[Y_1]^–$	Quercetin hexose–glucuronide
						465.1066	$[Y_1]^+$				301.0360	$[Y_0]^–$	
						303.0515	$[Y_0]^+$						
70	21.52	255, 352	551.1039	0.2	$C_{24}H_{23}O_{15}$	573.0847	$[M+Na]^+$	549.0879	–0.1	$C_{24}H_{21}O_{15}$	1099.1829	$[2M–H]^–$	Quercetin–3–*O*–malonylglucoside
						303.0508	$[Y_0]^+$				505.0987	$[M–H–CO_2]^–$	
						273.0406					463.0865	$[M–H–CO_2–C2H_2O]^–$	
						229.0497	$[Y_0–CHO–OH–CO]^+$				301.0340	$[Y_0]^–$	
						153.0186	$[^{1,3}A]^+$				300.0273	$[Y_0–H]^–$	
						145.0516	$[Y_0–CHO–OH–4CO]^+$				271.0243		
											255.0305	$[Y_0–CHO–OH]^–$	
											151.0038	$[^{1,3}A]^–$	
71	22.03	252, 364	551.1031	–0.6	$C_{24}H_{23}O_{15}$	573.0846	$[M+Na]^+$	549.0891	1.1	$C_{24}H_{21}O_{15}$	505.0990	$[M–H–CO_2]^–$	Quercetin–3–*O*–malonylglucoside
						303.0506	$[Y_0]^+$				463.0880	$[M–H–CO_2–C2H_2O]^–$	
						273.0407					301.0351	$[Y_0]^–$	
						229.0504	$[Y_0–CHO–OH–CO]^+$				271.0244		
						153.0196	$[^{1,3}A]^+$				255.0284	$[Y_0–CHO–OH]^–$	
						145.0495	$[Y_0–CHO–OH–4CO]^+$				151.0033	$[^{1,3}A]^–$	
											107.0130	$[^{0,2}A–2CO]^–;[^{0,2}B–CO]^–$	
72	23.69	–	551.1041	0.4	$C_{24}H_{23}O_{15}$	573.0851	$[M+Na]^+$	549.0894	1.4	$C_{24}H_{21}O_{15}$	505.0980	$[M–H–CO_2]^–$	Quercetin–3–*O*–malonylglucoside
						303.0504	$[Y_0]^+$				301.0335	$[Y_0]^–$	
						273.0768					300.0266	$[Y_0–H]^–$	
						229.0488	$[Y_0–CHO–OH–CO]^+$				271.0236		
						153.0195	$[^{1,3}A]^+$				255.0290	$[Y_0–CHO–OH]^–$	
						147.0456					151.0039	$[^{1,3}A]^–$	
											107.0127	$[^{0,2}A–2CO]^–;[^{0,2}B–CO]^–$	
73	11.51	253, 355	727.1348	–1.0	$C_{30}H_{31}O_{21}$	749.1142	$[M+Na]^+$	725.1176	–2.5	$C_{30}H_{29}O_{21}$	681.1274	$[M–H–CO_2]^–$	Quercetin–3–*O*–(6''–*O*–malonyl)–glucoside–7–*O*–glucuronide
						479.0830	$[Y_1]^+$				505.0977	$[M–H–CO_2–glucuronyl]^–$	
						303.0494	$[Y_0]^+$				301.0355	$[Y_0]^–$	
											255.0300	$[Y_0–CHO–OH]^–$	
74	13.82	253, 350	713.1565	0.0	$C_{30}H_{33}O_{20}$	735.1379	$[M+Na]^+$	711.1411	0.2	$C_{30}H_{31}O_{21}$	667.1519	$[M–H–CO_2]^–$	Quercetin–3–*O*–(6''–*O*–malonyl)–glucoside–7–*O*–glucoside
						465.1039	$[Y_1]^+$				463.0863	$[M–H–CO_2–hexosyl–C2H_2O]^–$	
						303.0508	$[Y_0]^+$				301.0348	$[Y_0]^–$	
											135.0641	$[^{0,2}A–CO]^–;[^{0,2}B]^–$	
75	12.18	–	627.1580	1.9	$C_{27}H_{31}O_{17}$	649.1414	$[M+Na]^+$	625.1391	–1.4	$C_{27}H_{29}O_{17}$	463.0874	$[Y_1]^–$	Quercetin–*O*–di–hexoside
						303.0502	$[Y_0]^+$				301.0344	$[Y_0]^–$	
						137.0611	$[^{0,2}A–CO]^+$						
76	16.07	–	627.1556	–0.5	$C_{27}H_{31}O_{17}$	649.1367	$[M+Na]^+$	625.1400	–0.5	$C_{27}H_{29}O_{17}$	447.0833	$[Y_1]^–$	Quercetin–*O*–rhamnosyl–gluconide
						449.1805	$[Y_1]^+$				301.0290	$[Y_0]^–$	
						303.0522	$[Y_0]^+$						
77	25.27	265, 347	535.1094	0.6	$C_{24}H_{23}O_{14}$	557.0905	$[M+Na]^+$	533.0889	–3.9	$C_{24}H_{21}O_{14}$	489.1039	$[M–H–CO_2]^–$	Kaempferol–3–*O*–(6''–*O*–malonyl)–glucoside
						287.0560	$[Y_0]^+$				285.0399	$[Y_0]^–$	
						121.0301	$[^{0,2}B]^+$				255.0298	$[Y_0–CO–2H]^–$	
						153.0204	$[^{1,3}A]^+$				227.0343	$[Y_0–CHO–CO–H]^–$	
											151.0037	$[^{1,3}A]^–$	
											107.0154	$[^{0,2}A–2CO]^–;[^{0,2}B–CO]^–$	
78	23.90	–	449.1092	0.8	$C_{21}H_{21}O_{11}$	471.0901	$[M+Na]^+$	447.0925	0.2	$C_{21}H_{19}O_{11}$	285.0410	$[Y_0]^–$	Kampferol–3–*O*–glucoside
						287.0561	$[Y_0]^+$				151.0056		

	LC	DAD	ESI(+)–QToF/MS					ESI(–)–QToF/MS					Assignment
Nº	Rt (min)	UV bands (nm)	Exp. Acc. Mass $[M+H]^+$	Error (mDa)	Formula $[M+H]^+$	Adducts & fragment ions of $[M+H]^+$ *m/z*		Exp. Acc. Mass $[M-H]^-$	Error (mDa)	Formula $[M-H]^-$	Adducts & fragment ions of $[M-H]^-$ *m/z*		Tentative identification
79	26.43	–	449.1084	0.0	$C_{21}H_{21}O_{11}$	471.0830	$[M+Na]^+$	447.0925	–0.1	$C_{21}H_{19}O_{11}$	285.0406	$[Y_0]^-$	Kaempferol–hexoside
						287.0549	$[Y_0]^+$						
80	22.34	265, 332	463.0878	0.1	$C_{21}H_{19}O_{12}$	485.0683	$[M+Na]^+$	461.0724	0.4	$C_{21}H_{17}O_{12}$	285.0403	$[Y_0]^-$	Kaempferol–3–*O*–glucuronide
						287.0559	$[Y_0]^+$				257.0471	$[Y_0–CO]^-$	
						133.1025	$[^{1,3}B–2H]^+$				229.0509	$[Y_0–2CO]^-$	
81	27.08	–	287.0560	0.4	$C_{15}H_{11}O_6$	259.1070	$[Y_0–CO]^+$	285.0399	0.0	$C_{15}H_9O_6$	153.0197	$[^{1,3}A]^-$	Kaempferol
						213.0885	$[Y_0–H_2O–2CO]^+$				137.0239	$[^{0,2}A–CO]^-;[^{0,2}B]^-$	
						185.0970	$[Y_0–H_2O–3CO]^+$				133.0310	$[^{1,3}B–2H]^-$	
						171.0856	$[Y_0–CHO–OH–CO–C2H_2O]^+$				109.0296	$[^{0,2}A–2CO]^-;[^{0,2}B–CO]^-$	
						153.0146	$[^{1,3}A]^+$				93.0340	$[^{0,2}B–CO]^-$	
						137.0894	$[^{0,2}A–CO]^+;[^{0,2}B]^+$						
						135.0776	$[^{1,3}B–2H]^+$						
						127.0807	$[Y_0–CHO–OH–3CO–CH_2O]^+$						
						121.0653	$[^{0,2}B]^+$						
						107.0500	$[^{1,3}A–H_2O–CO]^+$, $[^{1,3}B–CO]^+$						
						105.0681	$[^{1,3}B–2H–CO]^+$						
Flavones													
82	19.82	255, 347	449.1081	–0.3	$C_{21}H_{21}O_{11}$	471.0901	$[M+Na]^+$	447.0925	–0.2	$C_{21}H_{19}O_{11}$	895.1951	$[2M–H]^-$	Luteolin–7–*O*–glucoside
						371.1316					285.0400	$[Y_0]^-$	
						287.0559	$[Y_0]^+$				217.0505	$[Y_0–C2H_2O–C2H_2]^-$	
						153.0177	$[^{1,3}A]^+$				199.0396	$[Y_0–CHO–2CO–H]^-$	
						135.0821	$[^{1,3}B]^+$				175.0402		
83	17.45	253, 348	463.0880	0.3	$C_{21}H_{19}O_{12}$	485.0690	$[M+Na]^+$	461.0717	–0.3	$C_{21}H_{17}O_{12}$	923.1496	$[2M–H]^-$	Luteolin 7–*O*–glucuronide
						287.0559	$[Y_0]^+$				285.0398	$[Y_0]^-$	
						153.0186	$[^{1,3}A]^+$				217.0506	$[Y_0–C2H_2O–C2H_2]^-$	
											199.0390	$[Y_0–CHO–2CO–H]^-$	
											175.0358		
											151.0032	$[^{1,3}A]^-$	
											133.0287		
											133.0287	$[^{1,3}B]^-$	
84	20.27	–	595.1651	–1.2	$C_{27}H_{31}O_{15}$			593.1498	–0.8	$C_{27}H_{29}O_{15}$	285.0685	$[Y_0]^-$	Luteolin–7–*O*–rhamnosyl–hexoside
85	21.17	268, 351	595.1672	0.9	$C_{27}H_{31}O_{15}$	617.1484	$[M+Na]^+$	593.1498	–0.8	$C_{27}H_{29}O_{15}$	447.0604	$[Y_1]^-$	Luteolin–7–*O*–rutinoside
						449.1083	$[Y_1]^+$				285.0400	$[Y_0]^-$	
						371.1316							
						287.0557	$[Y_0]^+$						
86	20.57	–	447.0912	1.5	$C_{21}H_{19}O_{11}$	271.0608	$[Y_0]^+$	445.0763	0.8	$C_{21}H_{17}O_{11}$	269.0449	$[Y_0]^-$	Apigenin–glucuronide
87	23.02	259, 328	433.1137	–0.2	$C_{21}H_{21}O_{10}$	271.0610	$[Y_0]^+$	431.0972	0.6	$C_{21}H_{19}O_{10}$	269.0441	$[Y_0]^-$	Apigenin–glucoside
88	23.90	–	579.1711	0.3	$C_{21}H_{21}O_{10}$	433.1124	$[Y_1]^+$	577.1553	0.4	$C_{27}H_{29}O_{14}$	433.2084	$[Y_1]^-$	Apigenin–*O*–rhamnosyl–hexoside
						271.0605	$[Y_0]^+$				269.0446	$[Y_0]^-$	
89	26.99	–	839.3358	–2.0	$C_{40}H_{55}O_{19}$	271.0610	$[Y_0]^+$	837.3194	–1.3	$C_{40}H_{53}O_{19}$	269.0450	$[Y_0]^-$	Apigenin conjugate
90	27.08	–	287.0560	0.4	$C_{15}H_{11}O_6$	259.1070	$[Y_0–CO]^+$	285.0399	0.0	$C_{15}H_9O_6$	153.0197	$[^{1,3}A]^-$	Luteolin
						213.0885	$[Y_0–H_2O–2CO]^+$				137.0239	$[^{0,2}A–CO]^-;[^{0,2}B]^-$	
						185.0970	$[Y_0–H_2O–3CO]^+$						
						179.0649	$[^{0,4}B]^+$						
						153.0146	$[^{1,3}A]^+$						
						137.0894	$[^{0,2}A–CO]^+;[^{0,2}B]^+$						
						135.0776	$[^{1,3}B–2H]^+$						
						117.0767	$[^{1,3}B–H_2O]^+$						
						107.0500	$[^{1,3}A–H_2O–CO]^+$, $[^{1,3}B–CO]^+$						

	LC	DAD	ESI(+)–QToF/MS					ESI(–)–QToF/MS					Assignment
Nº	Rt (min)	UV bands (nm)	Exp. Acc. Mass $[M+H]^+$	Error (mDa)	Formula $[M+H]^+$	Adducts & fragment ions of $[M+H]^+$ *m/z*		Exp. Acc. Mass $[M-H]^-$	Error (mDa)	Formula $[M-H]^-$	Adducts & fragment ions of $[M-H]^-$ *m/z*		Tentative identification
Flavanones													
91	14.87	284, 329 sh	465.1026	–0.7	$C_{21}H_{21}O_{12}$	487.0830	$[M+Na]^+$	463.0882	0.5	$C_{21}H_{19}O_{12}$	287.0555	$[Y_0]^-$	Eriodictyol–*O*–glucuronide
						289.0715	$[Y_0]^+$				151.0037	$[^{1,3}A]^-$	
						153.0187	$[^{1,3}A]^+$				135.0452	$[^{1,3}B]^-$	
											107.0133	$[^{0,4}A]^-$	
Coumarins													
92	6.50	290, 340	341.0866	–0.7	$C_{15}H_{17}O_9$	363.0684	$[M+Na]^+$	339.0727	1.1	$C_{15}H_{15}O_9$	399.1273	$[M-H+AcO]^-$	Esculetin–6–*O*–glucoside
						179.0345	$[Y_0]^+$				177.0188	$[Y_0]^-$	
						133.0284	$[Y_0–CO–H_2O]^+$				133.0288	$[Y_0–CO_2]^-$	
						123.0456	$[Y_0–2CO]^+$				105.0336	$[Y_0–CO_2–CO]^-$	
93	7.31	–	179.0341	0.3	$C_9H_7O_4$	133.0292	$[M+H–CO–H_2O]^+$	177.0191	–0.3	$C_9H_5O_4$	149.0236	$[Y_0–CO]^-$	Dihydroxycoumarin
						123.0437	$[M+H–2CO]^+$				133.0288	$[Y_0–CO_2]^-$	
											105.0341	$[Y_0–CO_2–CO]^-$	
94	10.23	–	179.0344	0.0	$C_9H_7O_4$	133.0289	$[M+H–CO–H_2O]^+$	177.0192	–0.4	$C_9H_5O_4$	149.0222	$[Y_0–CO]^-$	Dihydroxycoumarin
						123.0452	$[M+H–2CO]^+$				133.0292	$[Y_0–CO_2]^-$	
											105.0344	$[Y_0–CO_2–CO]^-$	
95	12.02	296, 330	179.0339	0.0	$C_9H_7O_4$	133.0288	$[M+H–CO–H_2O]^+$	177.0187	0.1	$C_9H_5O_4$	133.0236	$[Y_0–CO_2]^-$	6,7–dihydroxycoumarin
						123.0421	$[M+H–2CO]^+$				105.0340	$[Y_0–CO_2–CO]^-$	
96	9.05	–	295.0518	–6.4	$C_{13}H_{11}O_8$	317.0241	$[M+Na]^+$	293.0295	0.2	$C_{13}H_9O_8$	177.0194	$[Y_0]^-$	Maloyl–dihydroxycoumarin
						179.0376	$[Y_0]^+$				149.0243	$[Y_0–CO]^-$	
						133.0286	$[Y_0–CO–H_2O]^+$				133.0284	$[Y_0–CO_2]^-$	
						123.0463	$[Y_0–2CO]^+$				105.0342	$[Y_0–CO_2–CO]^-$	
97	10.54	–	295.0510	–5.6	$C_{13}H_{11}O_8$	133.0288	$[Y_0–CO–H_2O]^+$	293.0296	0.1	$C_{13}H_9O_8$	177.0187	$[Y_0]^-$	Maloyl–dihydroxycoumarin
											149.0090	$[Y_0–CO]^-$	
											133.0286	$[Y_0–CO_2]^-$	
											105.0339	$[Y_0–CO_2–CO]^-$	
98	12.54	–	295.0541	–8.7	$C_{13}H_{11}O_8$	179.0348	$[Y_0]^+$	293.0299	–0.2	$C_{13}H_9O_8$	177.0189	$[Y_0]^-$	Maloyl–dihydroxycoumarin
						133.0446	$[Y_0–CO–H_2O]^+$				149.0139	$[Y_0–CO]^-$	
											133.0290	$[Y_0–CO_2]^-$	
											105.0343	$[Y_0–CO_2–CO]^-$	
Hydrolysable tannins													
99	27.09	–			$C_{30}H_{31}O_{12}$			581.1663	–0.4	$C_{30}H_{29}O_{12}$	295.0826	[4–hydroxyphenylacetichex–H–H_2O]$^-$	Tri–4–hydroxyphenylacetic acid–glucoside
											175.0391	[4–hydroxyphenylacetichex–H–H_2O–$C_6H_5CH_3CO$]$^-$	
											151.0392	[4-hydroxyphenylacetic–H]$^-$	
											143.0344	[4–hydroxyphenylacetichex–H–H_2O–$C_6H_5CH_2OHCO_2$]$^-$	
Lignan derivatives													
100	21.00	–			$C_{22}H_{27}O_8$			417.1569	–2.0	$C_{22}H_{25}O_8$	359.1021	$[M–H–2CH_3–CO]^-$	Syringaresinol
101	13.90	–			$C_{28}H_{37}O_{13}$	603.2055	$[M+Na]^+$	579.2075	0.3	$C_{28}H_{35}O_{13}$	417.1544	$[M–H–hexosyl]^-$	Syringaresinol–hexose
						383.1479	$[M+H–hexosyl–2H_2O]^+$				399.1437	$[M–H–hexosyl–H_2O]^-$	
102	18.97	–			$C_{28}H_{37}O_{13}$			579.2104	–2.6	$C_{28}H_{35}O_{13}$			Syringaresinol–hexose
103	19.63	–			$C_{28}H_{37}O_{13}$	603.2061	$[M+Na]^+$	579.2079	–0.1	$C_{28}H_{35}O_{13}$	417.1558	$[M–H–hexosyl]^-$	Syringaresinol–hexose
											399.1493	$[M–H–hexosyl–H_2O]^-$	
104	23.30	–			$C_{28}H_{37}O_{13}$	603.2059	$[M+Na]^+$	579.2075	0.3	$C_{28}H_{35}O_{13}$	417.1555	$[M–H–hexosyl]^-$	Syringaresinol–hexose
						383.1505	$[M+H–hexosyl–2H_2O]^+$				387.1104	$[M–H–hexosyl–2CH_3]^-$	
105	15.06	205, 280			$C_{30}H_{39}O_{14}$			621.2198	–1.5	$C_{30}H_{37}O_{14}$	417.1559	$[M–H–acetylhexosyl]^-$	Syringaresinol–acetylhexose
											402.1313	$[M–H–acetylhexosyl–CH_3]^-$	
											399.1447	$[M–H_2O]^-$	
											387.1058	$[M–H–2CH_3]^-$	

	LC	DAD	ESI(+)–QToF/MS				ESI(–)–QToF/MS					Assignment
Nº	Rt (min)	UV bands (nm)	Exp. Acc. Mass $[M+H]^+$	Error (mDa)	Formula $[M+H]^+$	Adducts & fragment ions of $[M+H]^+$ *m/z*	Exp. Acc. Mass $[M-H]^-$	Error (mDa)	Formula $[M-H]^-$	Adducts & fragment ions of $[M-H]^-$ *m/z*		Tentative identification
106	24.50	–			$C_{30}H_{39}O_{14}$		621.2183	0.0	$C_{30}H_{37}O_{14}$	417.1548	$[M-H-acetylhexosyl]^-$	Syringaresinol–acetylhexose
										402.1313	$[M-H-acetylhexosyl-CH_3]^-$	
										387.1078	$[M-H-acetylhexosyl-2CH_3]^-$	
										359.1111	$[M-H-acetylhexosyl-2CH_3-CO]^-$	
										181.0503	$[M-H-acetylhexosyl-2CH_3O-OH-C_6H_2-CHO-2(CH_2CH)]^-$	
										166.0268	$[M-H-acetylhexosyl-2CH_3O-OH-C_6H_2-CHO-2(CH_2CH)-CH_3]^-$	
										151.0044	$[M-H-acetylhexosyl-2CH_3O-OH-C_6H_2-CHO-2(CH_2CH)-2CH_3]^-$	
										123.0065	$[M-H-acetylhexosyl-2CH_3O-OH-C_6H_2-CHO-2(CH_2CH)-2CH_3-CO]^-$	
107	24.63	–			$C_{30}H_{39}O_{14}$		621.2181	0.2	$C_{30}H_{37}O_{14}$	417.1546	$[M-H-acetylhexosyl]^-$	Syringaresinol–acetylhexose
										402.1313	$[M-H-acetylhexosyl-CH_3]^-$	
										387.1074	$[M-H-acetylhexosyl-2CH_3]^-$	
										359.1084	$[M-H-acetylhexosyl-2CH_3-CO]^-$	
										181.0503	$[M-H-acetylhexosyl-2CH_3O-OH-C_6H_2-CHO-2(CH_2CH)]^-$	
										166.0269	$[M-H-acetylhexosyl-2CH_3O-OH-C_6H_2-CHO-2(CH_2CH)-CH_3]^-$	
										151.0041	$[M-H-acetylhexosyl-2CH_3O-OH-C_6H_2-CHO-2(CH_2CH)-2CH_3]^-$	
108	19.22	–			$C_{28}H_{39}O_{13}$		581.2239	–0.5	$C_{28}H_{37}O_{13}$	341.1392	$[M-H-hexosyl-CH_3COOH-H_2O]^-$	Dimethoxy–hexosyl–laricresinol
										329.1390	$[M-H-hexosyl-CH_3COOH-2CH_3]^-$	
109	19.39	–			$C_{28}H_{39}O_{13}$		581.2238	–0.4	$C_{28}H_{37}O_{13}$	359.1494	$[M-H-hexosyl-CH_3COOH]^-$	Dimethoxy–hexosyl–laricresinol
										341.1383	$[M-H-hexosyl-CH_3COOH-H_2O]^-$	
										329.1392	$[M-H-hexosyl-CH_3COOH-2CH_3]^-$	
110	19.82	–			$C_{28}H_{39}O_{13}$		581.2201	3.3	$C_{28}H_{37}O_{13}$	359.1445	$[M-H-hexosyl-CH_3COOH]^-$	Dimethoxy–hexosyl–laricresinol
										329.1392	$[M-H-hexosyl-CH_3COOH-2CH_3]^-$	
111	16.37	–			$C_{34}H_{49}O_{18}$		743.2742	2.0	$C_{34}H_{47}O_{18}$	581.2249	$[M-H-hexosyl]^-$	Dimethoxy–dihexosyl–laricresinol
										359.1494	$[M-H-2hexosyl-CH_3COOH]^-$	
										341.1383	$[M-H-2hexosyl-CH_3COOH-H_2O]^-$	
										329.1392	$[M-H-2hexosyl-CH_3COOH-2CH_3]^-$	

[a] Fragment ions produced in MS were named according to Ma et al. (1997)(Ma, Li, Van den Heuvel, & Claeys, 1997).

[b] Abbreviations: Caffeic, caffeic acid; Cafquin, caffeoylquinic acid; Caftar, caffeoyltartaric acid; DiHBZ, dihydroxybenzoic acid; DiHBZhex, dihydroxybenzoic acid-hexoside; DihydroCaf, dihydrocaffeic acid; Gallic, gallic acid; HBZ, hydroxybenzoic acid; hex, hexose; 4-hydroxyphenylacetic, 4-hydroxyphenylacetic acid; 4-hydroxyphenylacetichex, 4-hydroxyphenylacetic acid-hexoside ; Malic, malic acid; pCoumaric, *p*-coumaric acid; Quin, quinic acid; Tartaric, tartaric acid; sh, shoulder.

[c] Abundances of the fragment ions of caffeoylquinic acids in the negative mode are given in parenthesis.

Figure 1 revised

Click here to download Figure(s): FoodChem_Fig1_Alonso-Salces_revised.eps

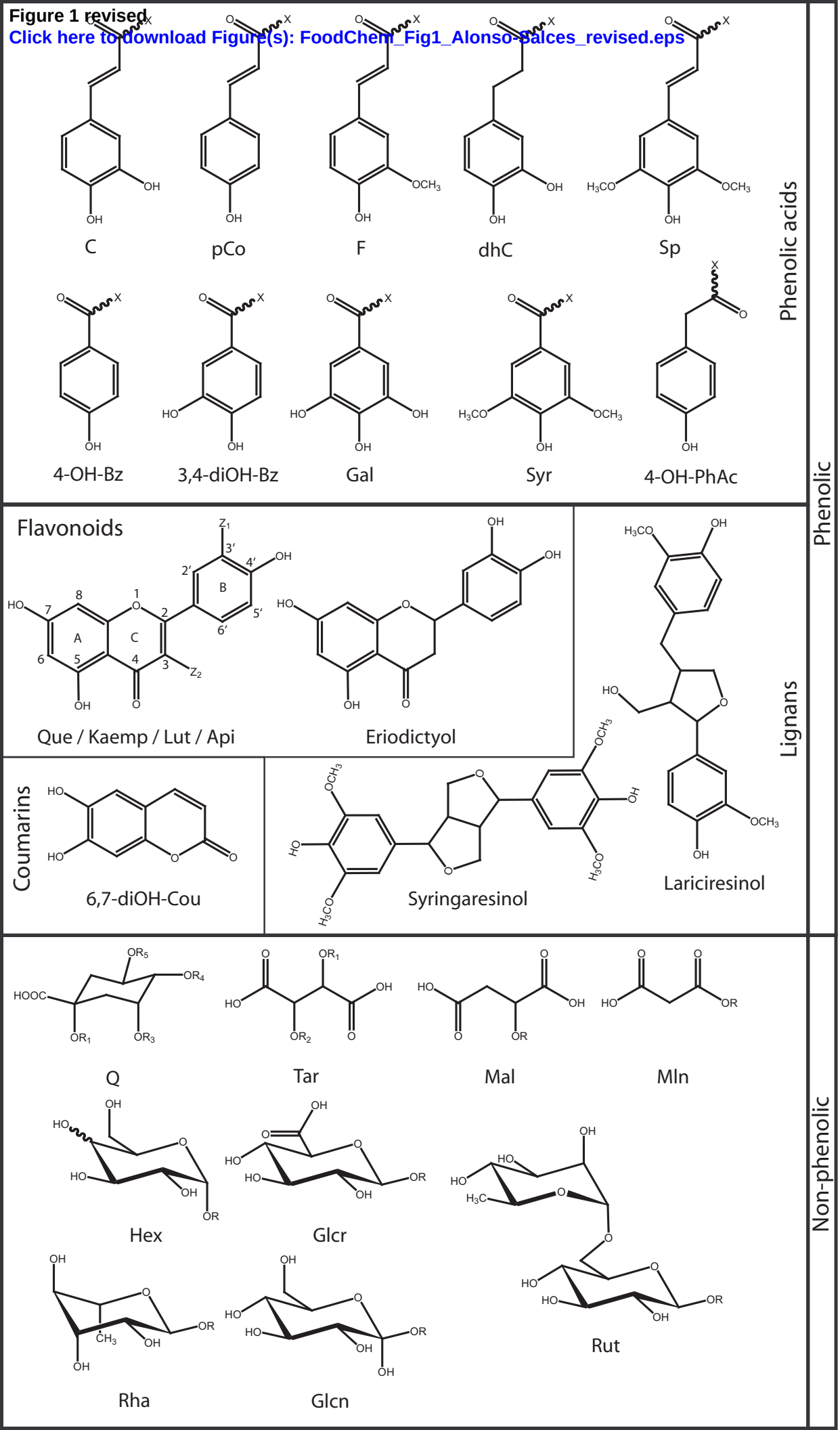

Figure 2

Click here to download Figure(s): FoodChem_Fig2_Alonso-Salces.eps

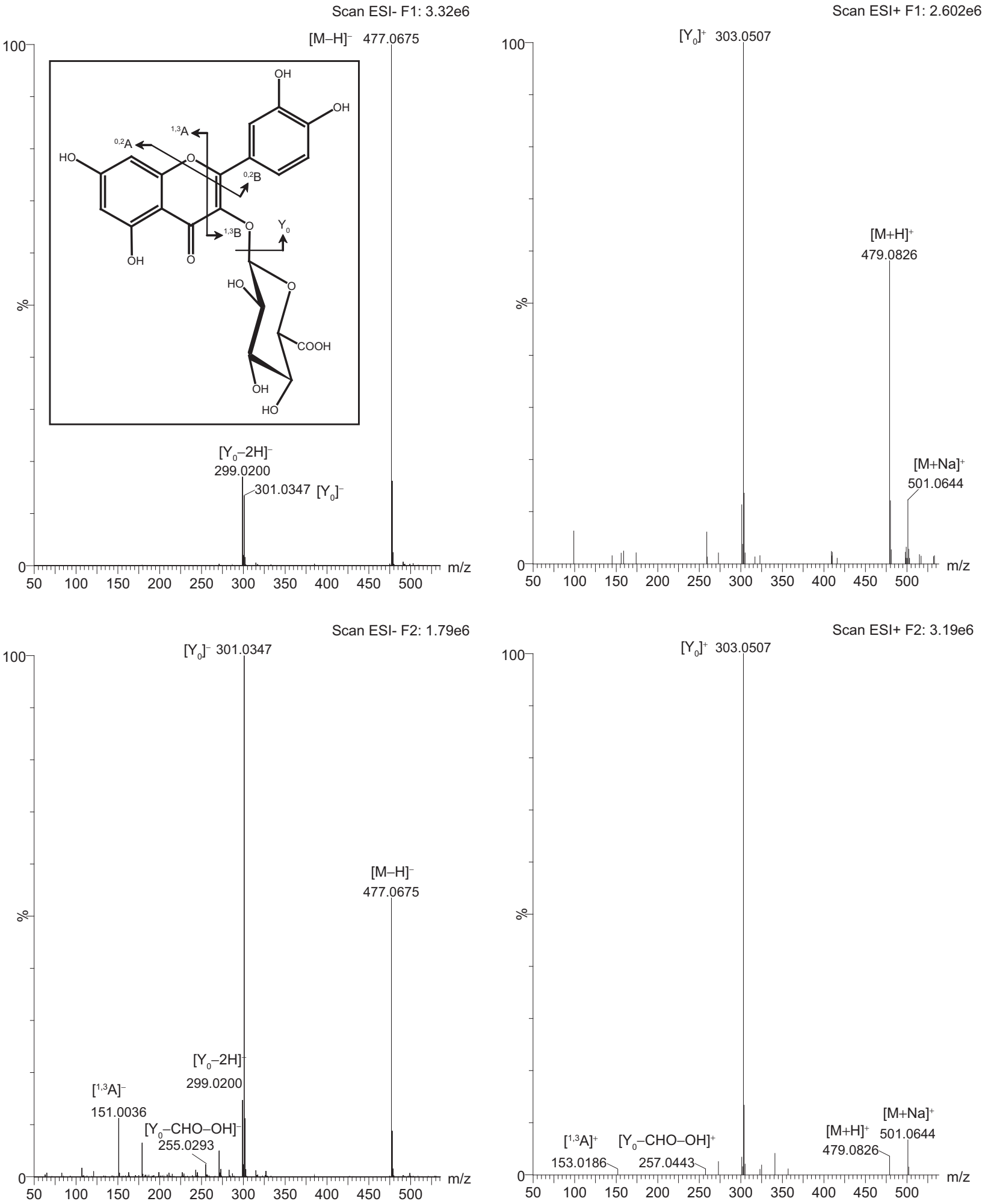

Figure 3
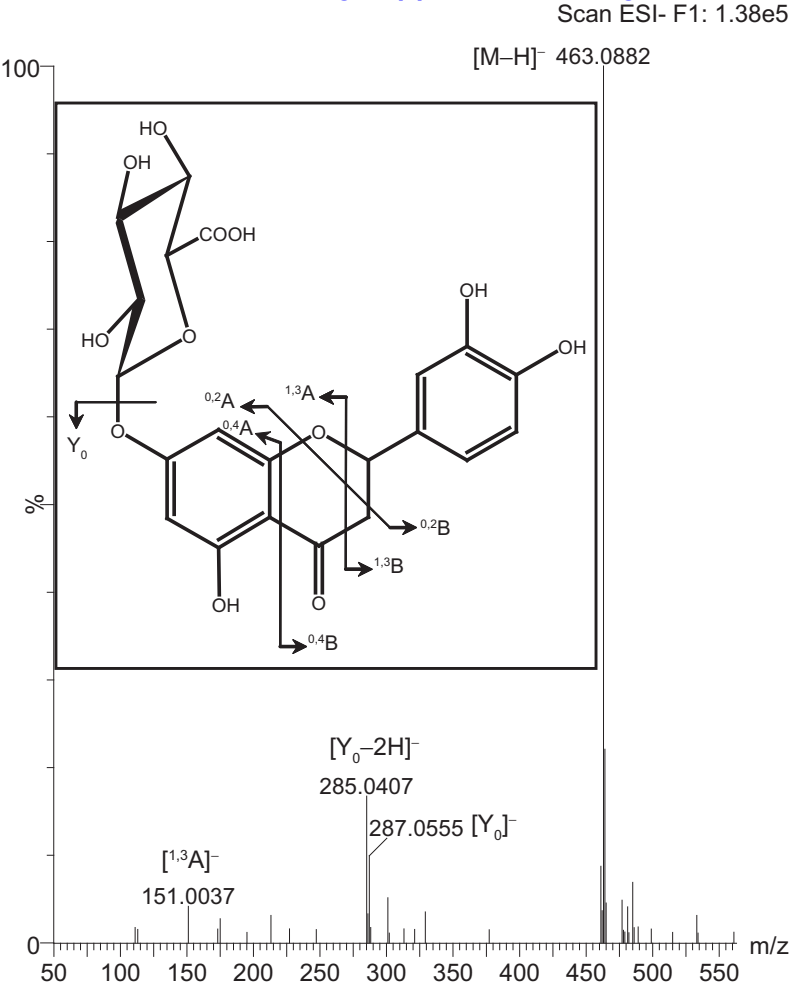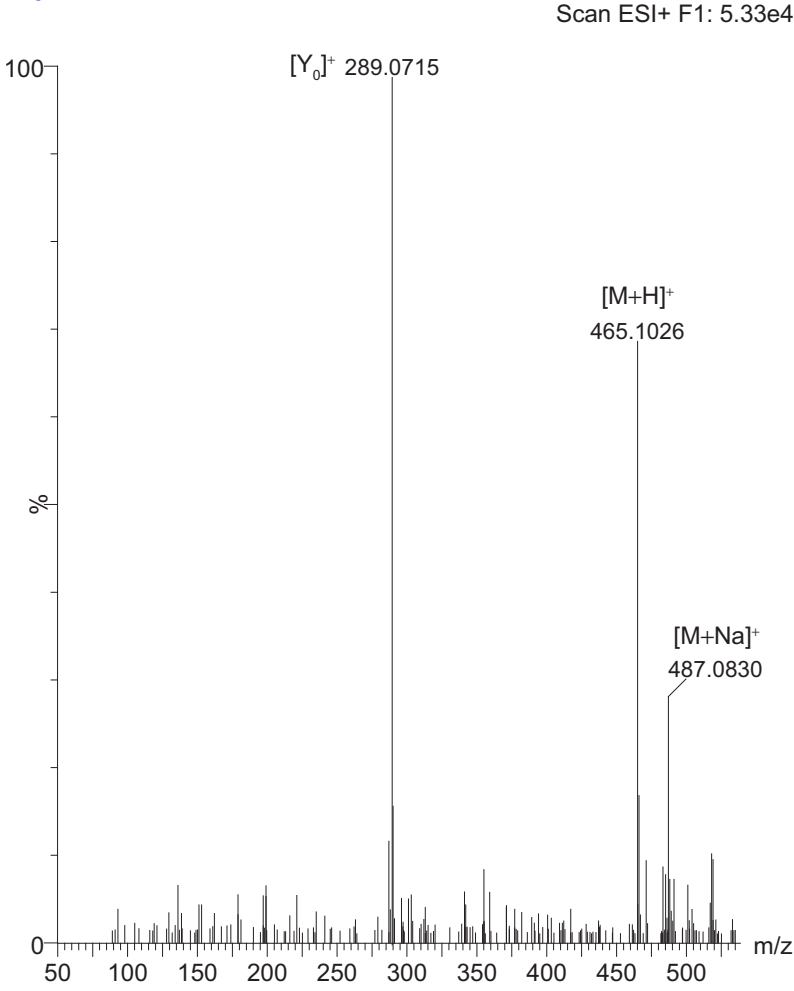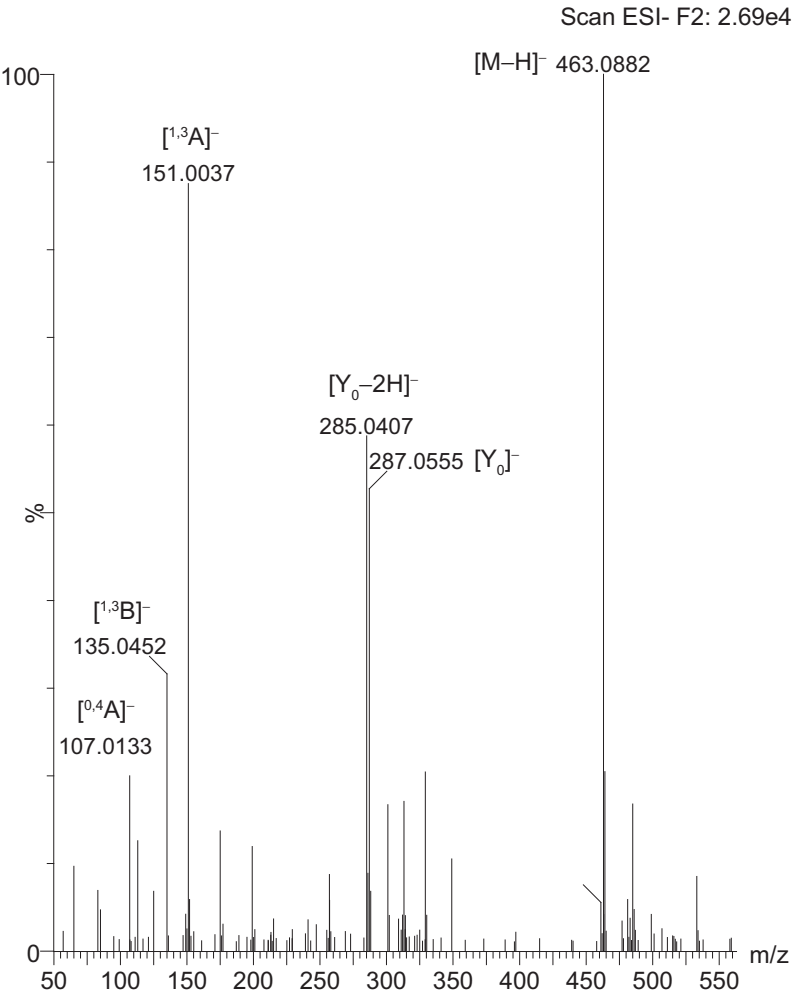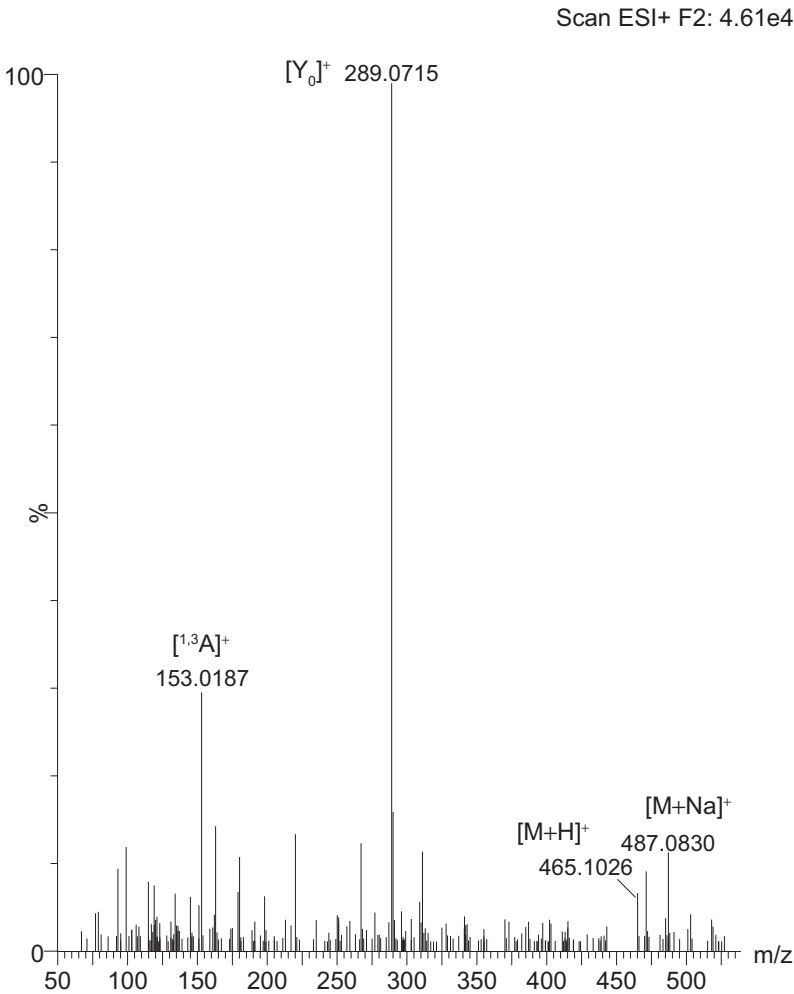
Click here to download Figure(s): FoodChem_Fig3_Alonso-Salces.eps